

FACILITY FORM 602

N69-39944	
(ACCESSION NUMBER)	(THRU)
117	1
(PAGES)	(CODE)
CR-106266	03
(NASA CR OR TMX OR AD NUMBER)	(CATEGORY)

JET PROPULSION LABORATORY
CALIFORNIA INSTITUTE OF TECHNOLOGY
PASADENA CALIFORNIA

Reproduced by the
CLEARINGHOUSE
for Federal Scientific & Technical
Information Springfield Va 22151

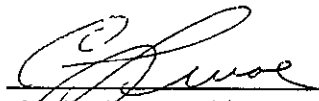
900-270


SURVEY AND STUDY FOR AN IMPROVED
SOLAR CELL MODULE

STOD TASK NO. 43

August 8, 1969

APPROVED BY


C. E. Levoe, Manager
Section 357


R. A. Marzek, Cognizant Engineer
Section 357
RESEARCHER

J E T P R O P U L S I O N L A B O R A T O R Y
C A L I F O R N I A I N S T I T U T E O F T E C H N O L O G Y
P A S A D E N A C A L I F O R N I A

PRECEDING PAGE BLANK NOT FILMED.

ABSTRACT

This document presents the results of the survey phase of STOD Task 43, Survey and Study for an Improved Solar Cell Module. STOD Task 43 is a program intended to determine what the state-of-the-art is with respect to silicon solar cell module fabrication, and where improvements can be made.

The initial survey phase consisted of seeking and collecting reports, documents, and other information to assist in determining what the state-of-the-art is in the design and manufacture of silicon solar cells. The information presented herein is the result of a review of documentation collected within the time limits allowed and includes only that information considered pertinent to what has been done, what is current practice and method, and what advanced planning is envisioned with respect to solar cell materials, fabrication methods, and processes.

The data is presented in seven sections with each section containing a summary of its contents. Items covered include: Cover glass, cover slip, integral cover glass, coatings, contacts, materials, adhesives, dielectrics, metallic coatings, interconnects, interconnect processes, and tests. Some design information and material compatibility studies are included. Recommendations are made for future programs.

ACKNOWLEDGMENT

The Researcher gratefully acknowledges the assistance given, in many forms, by JPL personnel and persons at the many companies contacted during the survey. Credits for material used herein are reflected in the References located throughout the text and on pages 7-3 and 7-4.

Additionally, the Researcher is most grateful to R. Ringsmuth, Co-researcher, for his work on Task 15, which provided the groundwork to this Task 43 effort and other information reflected in this document.

CONTENTS

I	INTRODUCTION	1-1
	1.1 PURPOSE OF SURVEY AND STUDY	1-1
	1.2 OBJECTIVES	1-2
	1.3 RESULTS	1-2
	1.4 CONCLUSION	1-3
	1.5 RECOMMENDATIONS	1-3
II	CELL PROTECTION AND EFFICIENCIES	2-1
	2.1 INTRODUCTION	2-5
	2.2 COVER GLASS	2-6
	2.3 FILTERS	2-8
	2.4 ANTI-REFLECTION COATINGS	2-11
	2.5 INTEGRAL GLASS COATINGS	2-14
III	CONTACTS	3-1
	3.1 ELECTROLESS-NICKEL PLATE	3-5
	3.2 SILVER TITANIUM	3-5
	3.3 SILVER CERIUM	3-6
	3.4 ALUMINUM AND NICKEL	3-7
	3.5 WRAPAROUND CONTACTS	3-12
	3.6 WRAPAROUND CELL FABRICATION	3-16
IV	MATERIALS	4-1
	4.1 SOLAR CELL ADHESIVES	4-5
	4.2 DIELECTRIC MATERIALS	4-11
	4.3 MISCELLANEOUS MATERIAL SYSTEMS	4-18
V	INTERCONNECTS	5-1
	5.1 INTRODUCTION	5-5
	5.2 INTERCELL CONNECTIONS	5-5
	5.3 INTERCONNECT DESIGNS	5-10
	5.4 DESIGNING OUT STRESSES	5-13
	5.5 INTERCONNECT MATERIALS	5-13

CONTENTS (Continued)

VI	INTERCONNECT PROCESSES AND SOLDERING MATERIALS	6-1
	6.1 INTRODUCTION	6-5
	6.2 REFLOW SOLDERING	6-5
	6.3 TUNNEL OVENS	6-11
	6.4 RESISTANCE WELDING	6-17
	6.5 ULTRASONIC BONDING	6-18
	6.6 INFRARED HEATING	6-21
	6.7 INDUCTION HEATING	6-25
	6.8 OTHER SOLDERING APPROACHES	6-27
	6.9 COMPARISON OF SOLDERING METHODS	6-27
	6.10 SOLDERING MATERIALS	6-27
VII	TESTS	7-1
	7.1 APPLICABLE TESTS	7-1
	REFERENCES	R-1
	APPENDIX A VERBAL CONTACTS	A-1
	APPENDIX B LIST OF DOCUMENTS COLLECTED	B-1
	APPENDIX C LIST OF MICROFILM REPORTS COLLECTED	C-1

TABLES

2-1	Relative performance, various solar cells and filters	2-10
2-2	Antireflection coating performance	2-13
2-3	Post-bombardment coating performance	2-14
2-4	Relative RF sputtering rates for various materials at several thousand volts peak-to-peak	2-19
3-1	Comparison of fabrication processes	3-5
3-2	Contact characteristics	3-6
3-3	Sputtered front aluminum contacts	3-8
3-4	Antireflected aluminum contacted cells	3-9
3-5	Cells with 2 micron evaporated aluminum	3-10
3-6	Nickel contact cells	3-11
3-7	Wraparound modules — Initial readings prior to thermal cycling	3-14
3-8	Wraparound modules — After 25 thermal cycles of -78.5°C to +60°C	3-15
4-1	Comparison of V_{OC} , P/langley/min before and after thermal soak test	4-7
4-2a	Weight loss after exposure to pressures of 5×10^{-6} to 5×10^{-7} torr and temperatures of 200°F to 250°F for 100 to 112 hours	4-8
4-2b	Weight loss after exposure to pressures of 5×10^{-6} to 5×10^{-7} torr and temperatures of 200°F to 250°F for 100 to 112 hours	4-9
4-3	Comparative tensile strengths of adhesive bonded aluminum specimens	4-10
4-4	Properties of cover glass adhesives	4-12
4-5	Properties of solar panel adhesives and primers	4-13
4-6	Properties of conductive adhesives	4-14

TABLES (Continued)

4-7	Test results summary	4-16
5-1	Physical and mechanical properties of metals used in solar cells	5-14
5-2	Materials and coatings used in interconnects (verbal contact source)	5-15
6-1	Some dissimilar-metal combinations that have been ultrasonically welded	6-21
6-2	Comparison of soldering methods	6-28
6-3	Comparison of Alpha 235 and 60/40 solder	6-32

FIGURES

2-1	Spectral emittance, various solar cells	2-6
2-2	Ultraviolet degradation of epoxy adhesive	2-7
2-3	Blue solar cell filter characteristics	2-9
2-4	Blue-red solar cell filter characteristics	2-10
2-5	Spectral reflectance, bare and coated solar cells	2-12
2-6	Relative spectral performance, bare and coated solar cells	2-12
2-7	RF sputtering process	2-18
3-1	High current high vacuum sputtering system schematic	3-7
3-2	14-Finger mask	3-8
3-3	Wraparound solar cell	3-13
3-4	RCA N/P silicon solar cell current-voltage characteristics	3-17
3-5	RCA N/P silicon solar cell current-voltage characteristics	3-18
3-6	RCA N/P silicon solar cell current-voltage characteristics	3-19
5-1	Rigid shingle	5-6
5-2	New interconnect approach	5-7
5-3	Solaflex interconnections using type AT-2010 cells	5-8
5-4	Solaflex interconnections using type AB-2020 cells	5-9
5-5	Submodule 2 x 2 cm cells x 6 cells wide	5-9
5-6	Submodule 2 x 6 cm cells x 2 cells wide	5-10
5-7	Interconnect configuration varieties	5-11
5-8	'P' Tab 612742 — after forming	5-12
5-9	'N' Bus bar 612738 — after forming	5-12
5-10	Submodule subassembly — before welding	5-12

FIGURES (Continued)

6-1	Single-point soldering	6-6
6-2	Parallel gap soldering	6-9
6-3	Profile development	6-13
6-4	Disassembled solder boat — early design	6-14
6-5	Disassembled solder boat — new design	6-14
6-6	Profile development — improved	6-16
6-7	Submodule subassembly before welding	6-17
6-8	Schematic diagram of traversing-table continuous-seam welding machine	6-20
6-9	Schematic of focused radiant heating system	6-23
6-10	Temperature versus time for infrared heating and typical soldering iron. The method of measurement is indicated by the sketch below the curves	6-24
6-11	Solubility of silver in tin-lead solders at various temperatures	6-31

SECTION I

INTRODUCTION

1.1 PURPOSE OF SURVEY AND STUDY

In the future, power demands upon solar cells will be in the multikilowatt range. To provide this power, when silicon solar cells are used, extremely large arrays are necessary. To build such arrays, an improved silicon solar cell module design is needed. This improved design would reflect the state-of-the-art in silicon solar cell module materials, methods, and processes.

Support to other Divisions (STOD) Task 43, "Survey and Study for an Improved Solar Cell Module" was initiated at the request of the Spacecraft Power Section (342) to determine the state-of-the-art, and where improvements can be made.

The program plan for STOD Task 43 was prepared by the Electronic Packaging and Cabling Section (357). This plan consisted of two phases: (1) a survey of the silicon solar cell industry, and (2) a study of the selected approaches to improve designs and processes. The survey phase consisted of extensive search and collecting of information in the following areas:

- 1) Research performed to develop, study, or advance solar cells even if it did not result in production of cells.
- 2) Designs of cells, cell modules, panels, and interconnects as used in flexible, rigid and hard cell applications.
- 3) Materials used in the fabrication module (or panel) including coatings, coverglass, interconnects, dielectrics, adhesives, solders, and the materials used to assist in the fabrication such as fluxes and cleaning solvents.
- 4) Fabrication including equipment, processes, methods, techniques, including various methods to join such as induction heating and reflow soldering.

- 5) Limitations such as operational parameters, vibrational extremes, and radiation effects.
- 6) Testing and qualification parameters, acceptance criteria, standards or other means of determining performance of completed cells, modules, and panels.

In addition, the information collected in a previous survey, STOD Task 15, is included.

1.2 OBJECTIVES

This document reports the results of the survey phase of the task. The intent of the survey is to determine what has been done, what is being done, and what is planned with respect to materials, methods, and processes.

1.3 RESULTS

The information reported herein represents approximately 20% of the information collected. The remaining 80% is not included because it was not received in sufficient time, with respect to the time required for review and preparation of this report. In this respect, the information contained in this report does not reflect the complete state-of-the-art as it exists today. It is estimated that an additional 20% of the information desired exists but is considered not available at this time. This includes programs-in-progress where no reports exist, company confidential information, classified programs involved, etc.

The personnel contacted at the various companies provided information as available to them, excluding proprietary or classified information. Where proprietary or classified information was involved, some personnel became exceedingly cautious and information given was sparse.

Most of the information was obtained from existing reports while verbal contacts provided insight into new processes. If the verbal contacts expressed sincere opinions, then some companies were working on identical processes under the impression that each is developing unique techniques for bonding solar cell electrical interconnections.

1.4 CONCLUSION

The area where advancement appears most promising is the processes for bonding the interconnects. Induction heating, infrared heating, and ultrasonic bonding all appear applicable to mass production automated fabrication techniques.

No materials were found to exhibit perfect properties for use as an interconnect. Until such an ideal material is found, trade-offs will be made between thermal and electrical properties.

1.5 RECOMMENDATIONS

It is recommended that a program be initiated to determine the differences, advantages, and disadvantages between induction heating, infrared heating and ultrasonic bonding. This could best be accomplished in two parts. The first part would permit complete freedom in the interconnect design and material selection to permit the evaluation of differences between the process capabilities. The second part would establish specific control parameters for the interconnect design and materials to be used to determine individual process flexibilities. Comparing the capabilities and flexibilities of these processes may lead to new insights into solar cell module interconnect design and material selection.

SECTION II
CELL PROTECTION AND EFFICIENCIES

Summary

- 2.1 Introduction
- 2.2 Cover Glass
- 2.3 Filters
- 2.4 Antireflection Coatings
- 2.5 Integral Glass Coatings

PRECEDING PAGE BLANK NOT FILMED.

SUMMARY

To achieve maximum efficiency, silicon solar cells must be protected from the effects of radiation. This protection has taken on the form of cover glass and filters. They aid in controlling the equilibrium temperature. Antireflection coatings are also used to increase, in percentage, the useful radiation penetrating the cell.

As a result, efficiencies have increased from 6% for the bare cell to as high as 14% for a protected cell with anti-reflection coatings when compared to a theoretical maximum of 25%.

SECTION II

CELL PROTECTION AND EFFICIENCIES

2.1 INTRODUCTION

Silicon solar cells are used to produce electrical energy by exposure to solar radiation. Most of the incident solar radiation is absorbed by the cell while a portion of it is reflected back into space. A small percentage of this absorbed radiation is converted into electrical energy and the remaining large portion is converted into heat. Some of this heat causes the cell to rise in temperature while the rest of it is reradiated out into space. When equilibrium temperature is reached, the absorbed radiation energy equals the sum of that radiation energy converted into electrical energy and the re-radiation energy. The problem is that the operating temperature has an inverse effect on the efficiency of the solar cell. The higher the temperature, the lower the efficiency.

Numerous efforts have been directed toward providing protection to the solar cells, thereby improving their efficiency while overcoming some of the problems associated with radiation. The requirements for the means of protection are the following:

- 1) Thickness enough to provide sufficient protection from the radiation environment.
- 2) Antireflective and non-absorbent in the wavelength range from 0.4 micron to 1.2 microns.
- 3) Reflective to the rest of the spectrum (if possible), particularly in the wavelength range from 1.2 microns to 4 microns.
- 4) Highly emissive in the wavelength range from 5 microns to infinity (Ref. 1).

In general, these include the use of cover glass, antireflection coatings, filters, and integral glass coatings.

This section covers the efforts reported by industry in the above mentioned areas.

2.2 COVER GLASS

One of the earliest approaches to the enhancement of solar cell emittance was the application of thin glass cover slides to the cell surface. Bare solar cells of the early P/N variety (P-type diffusion into an N-type base) have a room temperature emittance of about 0.32; borosilicate glasses have typical emittances of about 0.85. It, therefore, appeared reasonable to assume that the effective emittance of the solar cell could be raised by placing a glass slide in thermal contact with the active cell surface. Normal spectral emittance curves for bare and covered cells are shown in Fig. 2-1. Data are shown for fused silica covers as well as for microsheet glass covers.

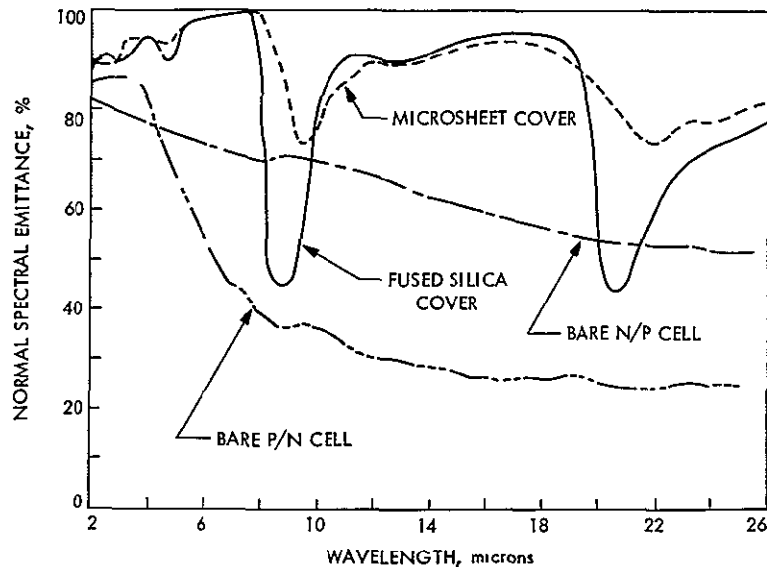


Fig. 2-1. Spectral emittance, various solar cells (Ref. 3) Note: bare N/P is SiO coated, bare P/N is not surface coated

The borosilicate glasses were used in a variety of thickness as low as 70 microminches, with the most common thickness being 150 microminches (Ref. 3).

Various techniques have been used to apply the covers to the cells. The Telstar satellite used mechanical means (Ref. 4). Epoxy adhesives with high optical transmission and good mechanical properties were available and were introduced as a means of attaching the cover glass to the cell in lieu of

the mechanical method. Adhesive thickness on the order of 25 microns were commonly used. The combination of a plain glass cover glass bonded to the cell with an adhesive provided a substantial gain in output (up to 34% increase for older P/N cells and a 7% increase for N/P cells) over the uncovered solar cells.

This new approach was not without problems. Microsheet glass transmits well through the near ultraviolet. Thus, most of the solar ultraviolet energy falls upon the epoxy adhesive. Laboratory tests have demonstrated that the effect of the ultraviolet upon the adhesive is a net loss of useful solar energy reaching the cell. Typical test results for one of the better epoxy adhesives are shown in Fig. 2-2.

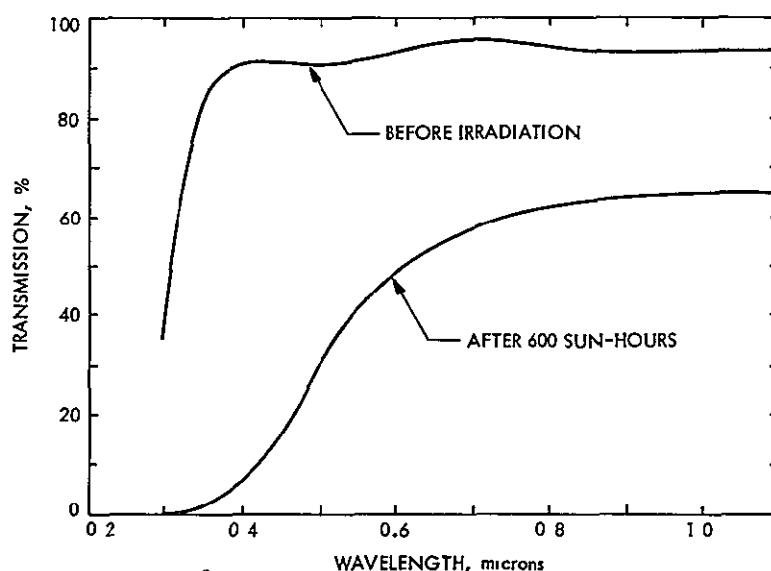


Fig. 2-2. Ultraviolet degradation of epoxy adhesive (Ref. 3)

New cover slide and adhesive materials were required as more was learned of the space environment. Certain spacecraft orbits and trajectories expose the vehicle to appreciable intensities of charged elementary particles. Included in this environment are the trapped protons and electrons of the natural or Van Allen belts, the trapped electrons introduced by high-altitude nuclear tests, and the high-energy protons produced by solar flare events. Because of the necessary exposure of the solar cell components, these

materials are also subject to possible damage from high-energy particles in the form of color center formations. Extensive test programs have shown certain glass cover materials to be superior to others. Microsheet glass (Corning 0211) was found to be quite susceptible to particle-induced discoloration.

Among the more superior materials evaluated were the vacuum deposited fused silicas (such as Corning 7940). Thus, fused silica has gradually replaced microsheet glass for most spacecraft missions (See Fig. 2-1).

2.3 FILTERS

Protection of the adhesive is obtained through the incorporation of ultraviolet, reflective coatings. Multilayer interference filters were then developed for deposition upon the glass cover slide so that they would reflect the ultraviolet energy before it could reach and damage the adhesive.

The optical properties of these interference filters as a function of wavelength, are dependent upon the number and arrangement of the layers, the index of refraction of each layer, and the physical thickness of each layer. The design of the filter is best handled using digital computer techniques once a general idea of the desired filter characteristics is established. The original requirement of the solar cell system engineer was that the filter should reflect almost all ultraviolet energy below the region of solar cell response. A filter with an abrupt cut-off of transmittance would best suit this requirement. Also, it was desirable to be able to obtain filters with different cut-on wavelengths so that solar cells with different spectral response characteristics could be accommodated. Filters with cut-on wavelengths of 400 microns to 450 microns are now commonly available.

The blue, reflecting filters thus developed by the coating industry proved quite satisfactory to the power system designer. Solar ultraviolet energy was effectively reflected before it could darken the transparent adhesive. The transmittance characteristics of a typical blue filter are shown in Fig. 2-3. This particular filter consists of 16 individual layers. It should be noted, however, that in the search for materials which would be less susceptible to electron and proton bombardment, transparent silicone potting compounds were adapted for use as cover adhesives. These materials proved to

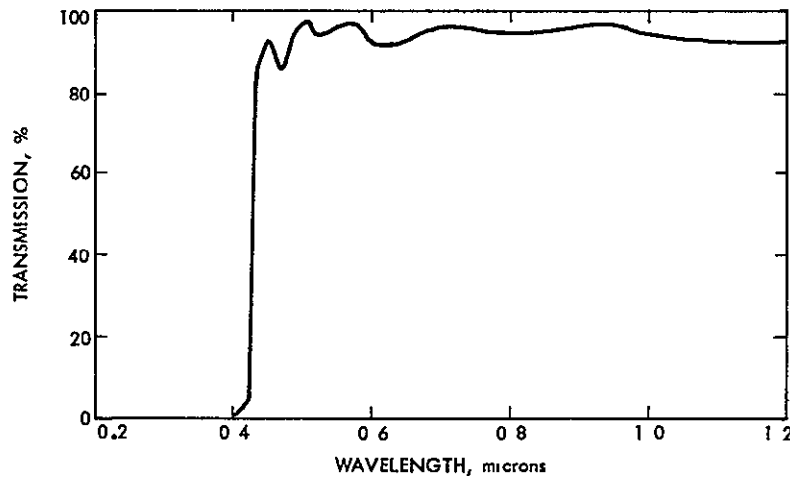


Fig. 2-3. Blue solar cell filter characteristics (Ref. 3)

be only slightly darkened by ultraviolet energy and unharmed by penetrating radiation.

In addition to protecting the adhesive, the blue filter can also be considered as a reflector of energy which would otherwise be absorbed without contributing to the solar cell output. If this energy were reflected, a slightly lower temperature would result, providing additional electrical power output. Since solar cells can be produced with a variety of spectral response properties dependent upon the N-layer diffusion process, an optimization of cell/filter characteristics is possible. Electrical power gains of up to 5% are available through the proper selection of blue filter cut-on wavelength for the particular cell being used. These gains are based on the reduction of cell temperature, and include transmission losses through the cover (Table 2-1).

The blue-red solar cell filter is one which provides a band of solar infrared reflectance in addition to the ultraviolet reflectance obtained in the blue filter. The characteristics of a typical 41-layer blue-red filter are shown in Fig. 2-4. The principle objective of this filter is to reflect as much solar energy as possible that is not contributing to the electrical output of the solar cell. The width of the reflection band can be made greater than shown;

Table 2-1. Relative performance, various solar cells and filters (Ref. 3)

Solar cell and test condition	Solar absorptance	Thermal emittance	Stabilization temperature, °C	Solar cell power output, mw
P/N solar cell No cover	0.93	0.32	89.4	16.9
N/P solar cell No cover	0.82	0.63	58.3	21.4
N/P solar cell Fused silica cover No filter	0.82	0.81	49.1	22.7
N/P solar cell Fused silica cover Blue filter	0.78	0.81	45.0	23.7
N/P solar cell Fused silica cover Blue-red filter	0.70	0.81	37.2	24.3
N/P solar cell Fused silica cover "Ideal" blue-red filter	0.65	0.81	27.4	25.7

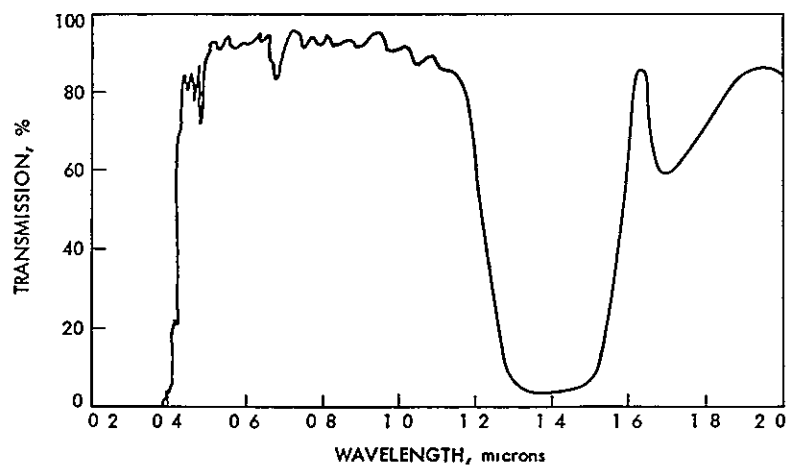


Fig. 2-4. Blue-red solar cell filter characteristics (Ref. 3)

however, the overall transmittance through the visible and near infrared consequently decreases. Thus, there is a limit to the feasibility of extending the reflection characteristics of the blue-red filter.

2.4 ANTI-REFLECTION COATINGS

The newer types of solar cells have highly polished surfaces for the purpose of improving diffusion characteristics. The reflectance of these surfaces is high enough to seriously decrease the apparent bare cell output under ground test conditions (Ref. 3).

Because of reflection, the available current of the non-coated cell is only 60% of the obtainable with an ideal non-reflecting silicon surface. In order to maximize the short-circuit current of cells, manufacturers apply antireflection coatings with thicknesses optimized to achieve minimum reflection in the 0.6- to 0.8-micron region. The coating factor, which is the ratio, expressed in percent, of coated-cell current to non-coated cell current, is a useful criteria of coating effectiveness (Ref. 2).

Although a thorough discussion on quarter-wavelength antireflection coatings will not be presented in this report, the basic requirements are provided for discussion. An antireflective coating for silicon solar cells should meet the following requirements:

- 1) High transmission in region of interest (0.4 to 1.2 microns)
- 2) Easily deposited at substrate temperature less than 350°C
- 3) Hard and adherent in deposited form
- 4) Insoluble in normal solvents (water, acetone, etc.)
- 5) Proper index of refraction (Ref. 4)

Figure 2-5 shows typical reflectance data for a bare cell and one employing a quarter-wavelength SiO₂ coating. The solar cell manufacturers have optimized the performance of their cells by selection of the coating thickness which best maximizes cell output. Coatings with thicknesses between 1100Å and 1400Å increase net current output by about 26%. As shown in Fig. 2-6 the SiO₂ coating contributes significantly to cell output, even with the application of a cover slide (Ref. 3).

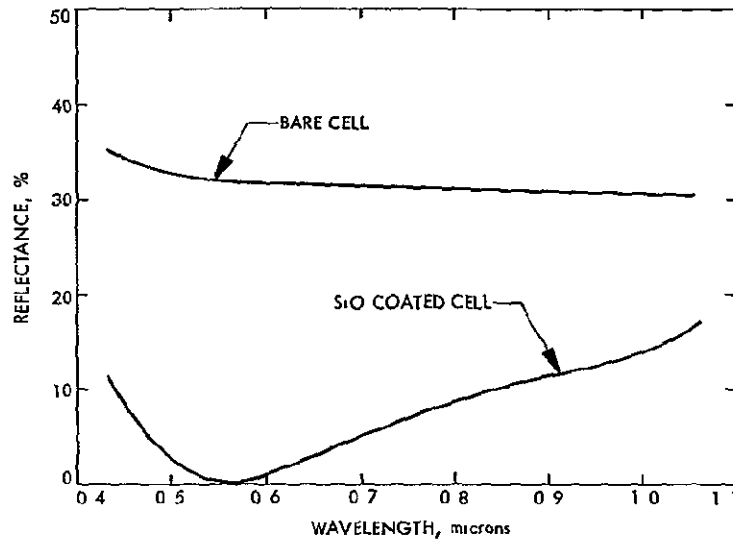


Fig. 2-5. Spectral reflectance, bare and coated solar cells (Ref. 3)

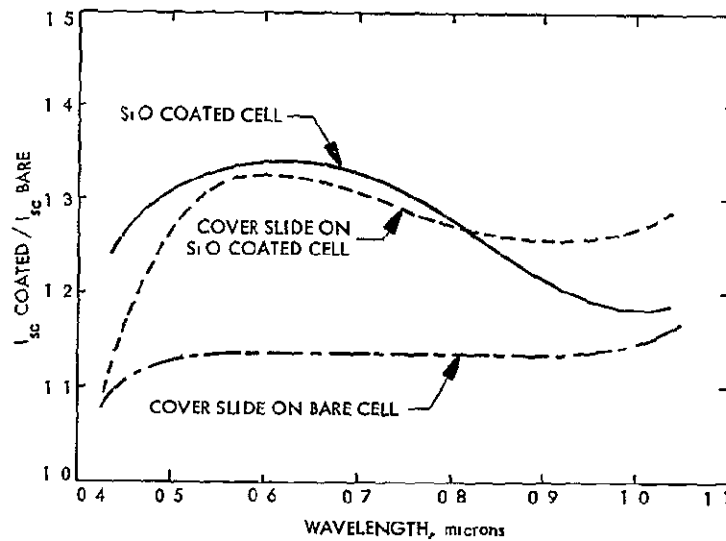


Fig. 2-6. Relative spectral performance, bare and coated solar cells (Ref. 3)

However, because silicon monoxide coatings can diminish reflection over only a restricted wavelength band, the corresponding coating factors of short wavelengths are often extremely low. The overall increase in short-circuit current obtained is 30%. The comparative effectiveness of the silicon

monoxide-magnesium fluoride coating can be judged from the superbue coating factors in Table 2-2. The super-blue coating was developed with the objective of achieving minimum reflection at short wavelengths. The interesting results are an increase in total short-circuit current of 40%, and the attainment of a coating factor of 178% at 0.4 micron: Coating factors obtained at 0.4 micron have ranged up to 195%. Such high coating factors are possible because reflection from silicon surfaces increases at short wavelengths.

Table 2-2. Antireflection coating performance (Ref. 2)

Filter wavelength, μ	Noncoated	Coated with SiO	Coating factor for SiO, %	Coated, superbue	Coating factor for superbue, %
Short-circuit current ^a , ma					
0.95	4.0	5.0	125	4.96	124
0.9	8.7	11.1	128	10.9	125
0.8	9.5	12.5	132	12.4	130
0.7	9.2	13.1	142	12.5	136
0.6	7.1	10.2	144	10.1	143
0.5	4.4	5.8	132	6.95	158
0.45	3.4	3.8	112	5.5	162
0.4	3.8	3.5	92	6.77	178
	Total 50.1	Total 65.0		Total 70.08	
Overall CF ^b	130			140	

^aMeasured with filter-wheel solar simulator, Ref. 6

^bCoating factor, CF = $\frac{\text{coated cell current}}{\text{noncoated cell current}} \times 100$; percent

An increase of the overall super-blue coating factor occurs with bombardment of the solar cell, as shown in Table 2-3. This increase is a consequence of the loss of long wavelength response of bombarded cells, whereas short wavelength response is unaltered. The high coating factors of the super-blue coatings at short wavelengths therefore improve this resistance to radiation damage of cells.

Table 2-3. Post-bombardment coating performance (Ref. 2)
(Post 1.5×10^{16} 1-Mev electrons)

Filter wavelength, μ	Noncoated	Coated with SiO	Coated, superblue
Short-circuit current, ma			
0.95	1.2	1.5	1.49
0.9	3.5	4.48	4.4
0.8	6.0	7.92	7.8
0.7	7.6	10.8	10.3
0.6	6.8	9.8	9.7
0.5	4.4	5.8	6.95
0.45	3.4	3.8	5.5
0.4	3.8	3.5	6.77
	Total 36.7	Total 47.60	Total 52.91
Overall CF, %		130	144

2.5 INTEGRAL GLASS COATINGS

Much effort has been devoted to the development of coatings which would provide the performance improvements of the cover slide/filter system at a reduced cost through a direct application to the solar cells themselves. These efforts have been concentrated in two areas: coatings which would increase the emittance of the cell surface and those which would reduce the reflectance of useful energy (Ref. 3).

The primary objectives for applying integral coatings to solar cells are as follows:

- 1) To eliminate adhesive between cell and cover glass (see Ref. 4).
Some of the reasons for this are:
 - a) The system is costly, present estimates for 2 cm² covers varying from \$0.50 to \$3.50, depending on the covers and filters required. When assembly costs are included, the cover costs can predominate in the completed solar array.
 - b) Despite much effort in adhesive selection, the adhesive sets the limit on mechanical strength and on environmental performance, particularly on the possibility of high temperature storage or operation (Ref. 5). Maximum temperature range is approximately 200°C. It has been demonstrated that radiation damage in silicon solar cells can be annealed out by subjecting the cell to approximately 400°C for brief periods (see Ref. 4).
 - c) The covers, especially those of thin glass are fragile and this complicates array assembly. The fragility adds much difficulty in providing covers thinner than 6 mils. For some missions, such thinner covers are sufficient and are of advantage in reducing the weight of the power supply (Ref. 5).
 - d) It removes the requirement for ultraviolet rejection filters on the underside of the cover glass.
- 2) To increase power-to-weight ratio of cell/cover glass assembly on missions which require less than 6-mil filters
- 3) To reduce the cost of present solar cell cover glass combinations (Ref. 4).

Numerous efforts have been extended developing a successful method of applying the integral glass cover directly to the silicon solar cell. The following is a partial list of some of these efforts

2.5.1 Fused Glass

NASA Contract NAS 5-3857 (May 4 to November 4, 1964) was a program to develop and produce integral glass coatings for solar cells. A limited amount of success was achieved with the coatings, which were applied in glass-slurry form and fused to the cell at a temperature between 850°C and 950°C. A major disadvantage of the procedure was that the solar cell diffusion and contact procedures had to be modified to prevent this high-temperature fusing cycle from drastically degrading the cells.

2.5.2 Spray Coatings

Spray coatings have been announced by Lockheed, but the advantages or exact properties of this coating are not explicitly known throughout the industry.

2.5.3 Thermal Decomposition

The thermal decomposition process involves passing an inert gas, as a carrying vapor, from the deposition agent over a heated substrate. The decomposing vapor deposits a film on the substrate. A large number of silanes have been used at Texas Instruments with deposition temperatures in the range of 400°C to 900°C. The major disadvantage of this technique is the relatively high deposition temperature and the relatively poor film quality for thick ($>10,000\text{\AA}$) depositions.

2.5.4 Reactive Sputtering

SiO_2 films in excess of 1.0 mil in thickness have been deposited on silicon by reactive sputtering. Silicon is used as the cathode in this process, and the sputtering operation in an oxygen-rich atmosphere deposits SiO_2 on the substrate.

Reactively sputtered SiO_2 can produce a thick film which is exceptionally smooth; however, sputtering rate must be kept below 200 Angstroms/min, and substrate temperature must be kept above 500°C. Consequently, 21 hours of continuous deposition would be required for producing a good film 1 mil in thickness. At higher deposition rates and lower substrate temperatures this process produces incompletely oxidized films of low density, thereby

limiting reactive sputtering, for most practical applications, to deposition of relatively thin films at high temperatures.

2.5.5 Electron-Beam Deposition

SiO_2 films in excess of 5.0 mils have been deposited by focused, electron beam techniques, using quartz as the source material. A major advantage of this technique is the substrate's relatively low temperature during deposition. Normally the substrate temperature may be below 50°C during the deposition to minimize thermal-stress problems. A disadvantage of this technique is the degree of control required to maintain a low evaporation rate in order to keep large particles of quartz from being evaporated. Highly strained films, which readily strip from silicon substrate, are commonly deposited with this technique unless a very low deposition rate (normally $< 300\text{\AA}/\text{min}$) is utilized.

2.5.6 High Vacuum Sputtering

NASA Contract NAS 5-10236 (starting date, June 1966) was initiated to investigate integral cover glass techniques for silicon solar cells. Several deposition techniques have been investigated during this contract, but the best reported results were obtained by high-vacuum sputtering. This technique has reportedly yielded films with excellent optical and mechanical characteristics, however, the rate at which the films are deposited is very low (average SiO_2 deposition rate is $100\text{\AA}/\text{min}$).

2.5.7 RF Sputtering

It has been demonstrated at Texas Instruments that complex thin films, such as pyrex, deposited by RF sputtering have physical and chemical properties basically identical with the parent bulk material. The RF sputtering process (Fig. 2-7) has the advantage of high deposition rates ($> 1000\text{\AA}/\text{min}$ for SiO_2) and low substrate temperatures ($< 200^\circ\text{C}$). RF deposited integral quartz films of 1- to 2-mil thickness have successfully passed five thermal shock cycles from -196°C to $+100^\circ\text{C}$ with no mechanical or physical deterioration or delamination from the solar cell.

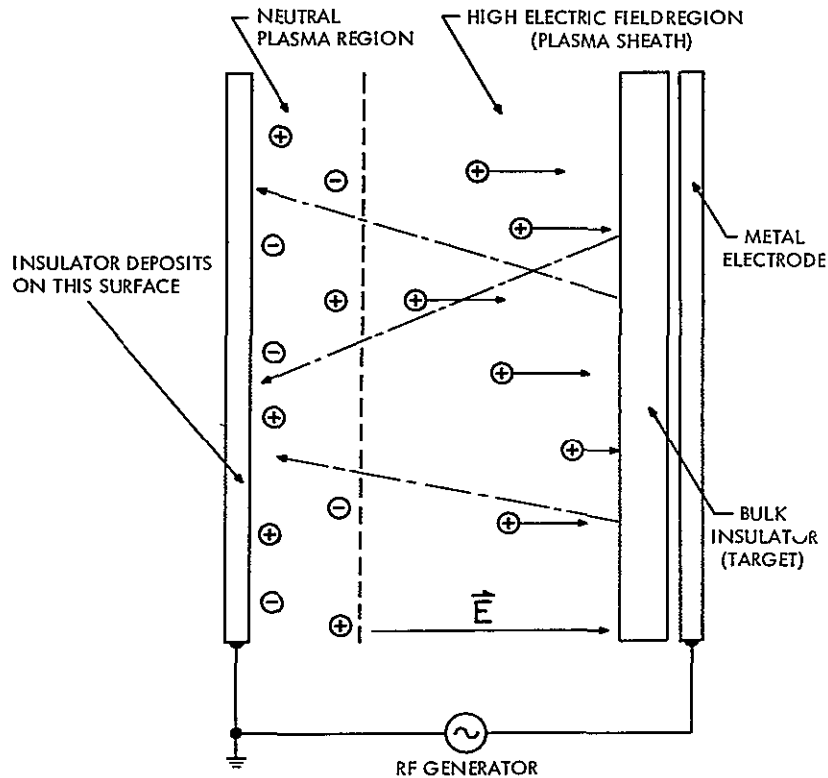


Fig. 2-7. RF sputtering process (Ref. 4)

Applications of radio-frequency sputtering to insulators have produced excellent results unattainable by any other method. Deposition rates for silica (SiO_2) of $200\text{\AA}/\text{min}$ have been achieved with excellent film properties. Table 2-4 shows some of the various types of glasses and other insulators which have been deposited by RF sputtering (Ref. 4).

As can be seen by the above processes, integral glass coating may be considered still in the experimental stages.

Table 2-4. Relative RF sputtering rates for various materials
at several thousand volts peak-to-peak (Ref. 4)

Material	Composition	Relative rates
Fused quartz	SiO_2	1.0
GSC-1 glass	5% Al_2O_3 , 10% B_2O_3 , 85% SiO_2	0.58
Pyrex 7740	80.5% SiO_2 , 12.9% B_2O_3 , 3.8% Na_2O , 2 2% Al_2O_3 , 0.4% K_2O	0.42
191 CP glass	16% Al_2O_3 , 7% CaO , 77% SiO_2	0.30
Alumina	Al_2O_3	0.30
Mullite	$\text{Al}_6\text{Si}_2\text{O}_{13}$	0.30
Boron nitride	BN	0.25

SECTION III

CONTACTS

Summary

- 3.1 Electroless-Nickel Plate
- 3.2 Silver Titanium
- 3.3 Silver Cerium
- 3.4 Aluminum and Nickel
- 3.5 Wraparound Contacts
- 3.6 Wraparound Cell Fabrication

PRECEDING PAGE BLANK NOT FILMED.

SUMMARY

Contacts used on solar cells to provide the electrical junction have undergone little improvement over the years, the only major change being from plated-gold-nickel as used on the P/N cells, to the silver-titanium contacts as used on the N/P cells. Silver cerium was determined to be superior for cells with integral cover glass. Recent efforts have resulted in aluminum and in nickel being tested as contacts, using sputtering techniques. A new approach using wrap-around contacts has also been fabricated with limited success.

SECTION III

CONTACTS

3.1 ELECTROLESS-NICKEL PLATE

Low resistance ohmic contacts were obtained through the exercise of extreme care in cleaning of the surfaces and of strict control of the plating process. This process was not suitable for N on P cells because of the polished surfaces involved.

3.2 SILVER TITANIUM

Production of N on P cells required the introduction of several new fabrication processes. The fabrication processes for the N on P cells are compared with those of P on N cells in Table 3-1. The processes for creating the P-N junction, for applying the contacts, and for decreasing the surface reflection differed so radically from those used for the P on N cell that it took several years for solar cell manufacturers to produce N on P cells on an economically sound basis (Ref. 2).

Table 3-1. Comparison of fabrication processes (Ref. 2)

Material	N on P	P on N
	P Type 0.5 to 1.2 ohm-cm	N Type 0.3 to 1.5 ohm-cm
Diffusion process		
Source	P_2O_5	$B Cl_3$
Temperature	875°C	1060°C
Time	30 min	10 min
Contact process	Evaporated, silver-titanium, sintered at 600°C	Plated, gold-nickel
Antireflection coating process	Evaporated SiO	Formed automatically in diffusion process

The advantages of Ti-Ag contacts were immediately recognized and, more recently, the disadvantages. This system is not giving the environmental stability and shelf life required.

Solder coating of the Ti-Ag contacts has retarded the degradation, or at least made the problem difficult to detect. The disadvantages of solder coated cells are the limited temperature range and the increase in weight (Ref. 6).

3.3 SILVER CERIUUM

During the development of integral cover glass on silicon solar cells, the characteristics of the junction were found to be degraded. The cause was determined to be the titanium in the Ti-Ag contacts as a result of the sintering process. Cerium was substituted for titanium and the problem, as reported, was resolved. The silver cerium contacts were considered superior to the silver titanium contacts as a result of tests performed and reported in Table 3-2 (Ref. 2).

Table 3-2. Contact characteristics (Ref. 2) (Contacts to extremely shallow junction cells)

Characteristic	Silver-Titanium	Silver Cerium
Slope ^a , R_c , ohms	0.25	0.2
"N" value	3-5	1.2-1.4
Diode reverse current ^b , I_R , A	100	20
Open-circuit voltage, V_{OC} , V	0.52	0.54
Break load, g	500	1500

^aSlope of forward biased diode voltage-current curve in 300 to 400 ma region.

^bDiode reverse current for 0.6-v bias.

It is of interest that with titanium silver contacts, the irradiation degradation could be recovered by a single firing at 605°C for 5 min. This type of contact has added versatility to damage-annealing studies. If annealing of highly damaged cells should be required, the front contacts developed in this work should allow the use of more severe annealing cycles (Ref. 5).

3.4 ALUMINUM AND NICKEL

Efforts were initiated to improve the known methods of establishing electrical contacts to silicon solar cells. The contact materials under investigation were aluminum (Al), nickel (Ni) and copper (Cu). One technique used was IPCs high-vacuum sputtering system (Fig. 3-1). The results of these efforts are given in 3.4.1 through 3.4.2, following.

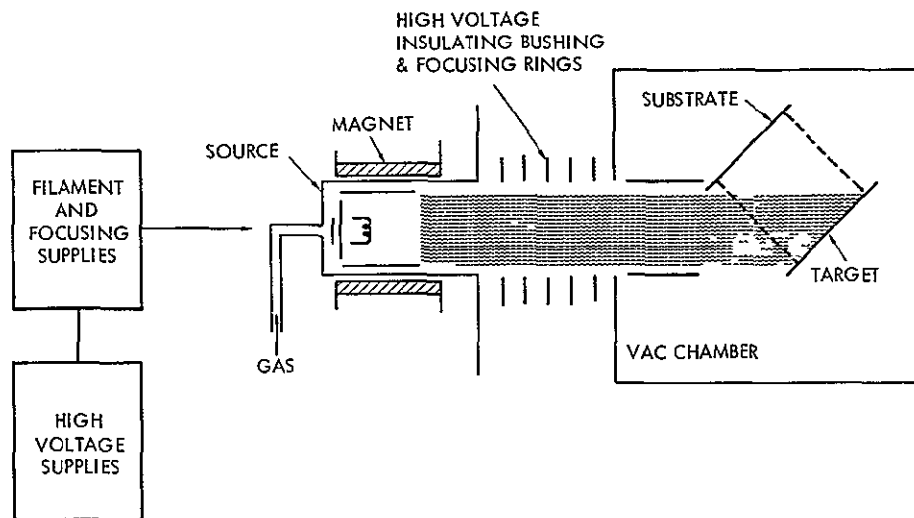


Fig. 3-1. High current high vacuum sputtering system schematic (Ref. 6)

3.4.1 Aluminum Contacts – High Vacuum Beam Sputtering

Both aluminum front finger contacts and back area contacts have been applied to IPCs N-on-P silicon solar cells. For the front contacts, IPCs standard 14-finger contact mask was used. The bimetallic mask was heated to 150°C which results in well-defined contact fingers as shown in Fig. 3-2. The fingers are tapered which is not indicated. The back surface contacts were deposited at room temperature.

Front contacts were applied with Al thickness from 1 to 5 microns. The back contact was approximately 2 microns thick. Finger resistance of front contacts is measured with an ohmmeter for approximately two-thirds of the length of the finger contact. Normal Ti-Ag cells measured by this technique are found to have finger resistances of less than 5 ohms. For the group of cells

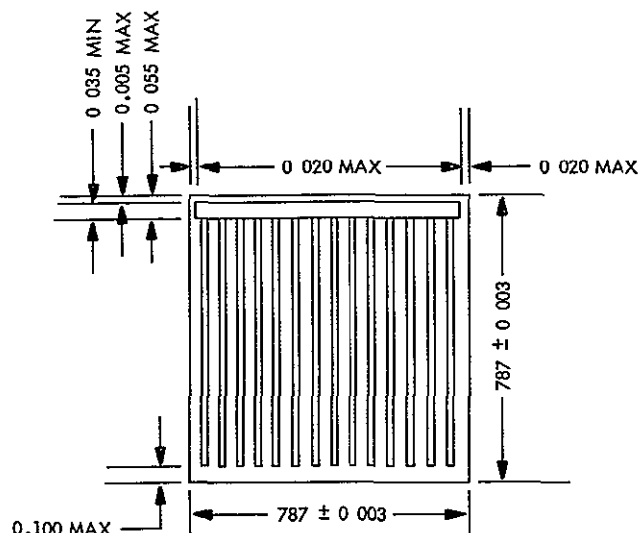


Fig. 3-2. 14-Finger mask (Ref. 6)

with 2 microns of Al, the finger resistance was found to be generally over 6 ohms. Another group of cells with 5 microns of Al on the front contact reduced the finger resistance to 5 ohms, but mechanical contact was poor.

Tape tests using Scotch Brand No. 810 were made of all Al contacted cells. All of the cells with 2 microns of Al passed the tape test without any noticeable removal of Al. As mentioned, the cells with 5 microns of Al were susceptible to peeling. Only 4 of the 10 cells tested did not indicate any peeling. The peeling started primarily at the contact bar during scribing of the cells to size. Electrical tests of these four cells are presented in Table 3-3.

Table 3-3. Sputtered front aluminum contacts (Ref. 6)
(No anti-reflection coating)

	I_{SC}	$I_{.43}$	V_{OC}
1	96	24	0.540
2	105	47	0.522
3	97	46	0.538
4	69	--	0.530

The electrical characteristics of the 20 cells fabricated with 2 microns of Al are indicated in Table 3-4. The table indicates results before and after a one-hour heat treatment cycle at 450°C. Initially a low open circuit voltage was found for a number of the cells which was improved for some of the cells by the temperature cycle. A threshold temperature for this improvement had been seen previously at 200°C, but in this test the improvement was not noticed until approximately 400°C. No further improvement was observed at 500°C.

Table 3-4. Antireflected aluminum contacted cells (Ref. 6)
(2 x 2 cm cells)

	Before anneal			After 450°C anneal		
	I_{SC}	$I_{.43}$	V_{OC}	$I_{.43}$	V_{OC}	$\eta\%$
1	128	112	0.548	114	0.549	9.2
2	129	120	0.550	121	0.550	9.8
3	131	125	0.550	125	0.550	10.1
4	126	76	0.513	120	0.545	9.7
5	124	93	0.532	116	0.544	9.4
6	126	64	0.496	105	0.520	8.5
7	127	86	0.520	98	0.517	7.94
8	129	116	0.540	121	0.546	9.8
9	130	112	0.534	119	0.562	9.6
10	132	119	0.546	122	0.552	9.9
11	127	76	0.516	106	0.529	8.57
12	124	100	0.532	115	0.540	9.30
13	128	40	0.488	109	0.531	8.80
14	128	113	0.532	122	0.543	9.90
15	132	85	0.510	121	0.540	9.80
16	126	106	0.531	118	0.544	9.55
17	132	121	0.549	125	0.551	10.1
18	134	118	0.543	122	0.548	9.9
19	122	78	0.546	89	0.545	6.7
20	130	103	0.547	119	0.547	9.6

It appears from the threshold observed that two distinct mechanisms are involved, although they are not fully understood.

Humidity chamber tests were carried out in IPCs Tenney chamber, which maintained at 60°C and 95% humidity. This is less than the contract requirement, but was believed to be adequate for initial testing. Cells were prepared with sputtered Al front contact and regular T₁-Ag back contacts. After one week, cells passed tape test with Scotch Brand No. 810 and no degradation was observed. After five weeks of testing, extensive peeling of the T₁-Ag back contact resulted in a stop testing. At that time the front Al contact passed the tape test.

3.4.2 Aluminum Contacts - Evaporation/Sintering

Another approach to the Al contacting problem is being carried out at IPC on Contract No. F33615-68-C-1164. Al contacts are being evaporated and sintered at slightly below the 577°C Al-Si eutectic. When the eutectic is reached, the alloy penetrates the junction and increased leakage degrades the cell. The firing at slightly below the eutectic does not appear to give excessive leakage, but does increase the bond strength. It has not been determined if the bond strength is adequate, but it appears to be comparable with the sputtered contacts fabricated on this program. The electrical characteristics are presented on Table 3-5.

Table 3-5. Cells with 2 micron evaporated aluminum (Ref. 6)

	Before CeO ₂ Coating			After CeO ₂ Coating		
	I _{SC}	I _{.43}	V _{OC}	I _{SC}	I _{.43}	V _{OC}
1	101	94	0.545	133	107	0.547
2	101	95	0.544	134	109	0.547
3	104	95	0.543	136	111	0.548
4	100	94	0.547	132	100	0.548

A 550°C sintering for 20 min had worked for evaporated cells as indicated above, the same treatment was used for the 5-micron sputtered Al contacts which had indicated poor efficiencies. In this case, the cells completely degraded, resulting in very low open circuit voltages.

3.4.3 Nickel Contacts - High Vacuum Beam Sputtering

Solar cells were fabricated with sputtered Ni contacts to both surfaces. Thick Ni contacts have indicated strain problems resulting in peeling, therefore, initial cells were made with 0.7 micron of Ni. This thickness of nickel will result in series-resistance problems.

These cells were being fabricated for delivery to JPL in April 1968. During the cleaning step prior to CeO_2 antireflection coating, damage to the contact was observed and resulted in the loss of part of the lot. The cleaning step involved ultrasonic cleaning in an alconox solution.

The electrical results for the cells (Ref. 6) are indicated in Table 3-6.

Table 3-6. Nickel contact cells
(0.7 micron Ni both surfaces by sputtering)
2 x 2 cm cells (Ref. 6)

	Before CeO_2			After CeO_2		
	I_{SC}	$I_{.43}$	V_{OC}	I_{SC}	$I_{.43}$	V_{OC}
1	97	44	0.496	117	46	0.516
2	97	50	0.514	124	56	0.521
3	87	29	0.490	101	39	0.515
4	91	50	0.516	128	59	0.525
5	97	48	0.516	130	64	0.525
6	100	52	0.509	121	76	0.513
7	96	39	0.489	112	40	0.527
8	93	37	0.496	117	54	0.541
9	98	53	0.522	127	58	0.523
10	94	32	0.492	116	52	0.529

Table 3-6. Nickel contact cells
(0.7 micron Ni both surfaces by sputtering)
2 x 2 cm cells (Ref. 6) (contd)

	Before CeO ₂			After CeO ₂		
	I _{SC}	I _{.43}	V _{OC}	I _{SC}	I _{.43}	V _{OC}
11	97	50	0.518	124	52	0.513
12	100	47	0.517	124	52	0.517
13	96	25	0.467	124	54	0.514
Avg I _{SC} before CeO ₂ = 95.6 ma Avg V _{OC} before CeO ₂ = 0.503 v Avg I _{SC} after CeO ₂ = 120.5 ma Avg V _{OC} after CeO ₂ = 0.521 v						

3.5 WRAPAROUND CONTACTS (Ref. 7)

Wraparound solar cells (both contacts on the back), Fig. 3-3, have been successfully fabricated. These cells have a 5% greater active area than cells of the standard construction. Because of this increase in area (5%) of the active surface of the cell, an increase in power output (5% max) for the same occupied area can be obtained. The use of these cells in the construction of modules employing printed circuit substrates has also been demonstrated. The efficiencies indicated for these modules (Tables 3-7 and 3-8) are slightly higher (0.4%, taking into account active area) than a module constructed of standard cells, such as the nimbus type. Examination of the power output shows an increase above the nimbus type module. The increase in power is not all due to an increase in efficiency. In fact, the power output of the wraparound module is 4% higher than the nimbus type after all factors have been taken into account. This is close to the expected 5% increase due to the area.

Problems have substrates were encountered. This area should be investigated to determine the best substrate arrangement, considering both weight as well as bonding strength of metals.

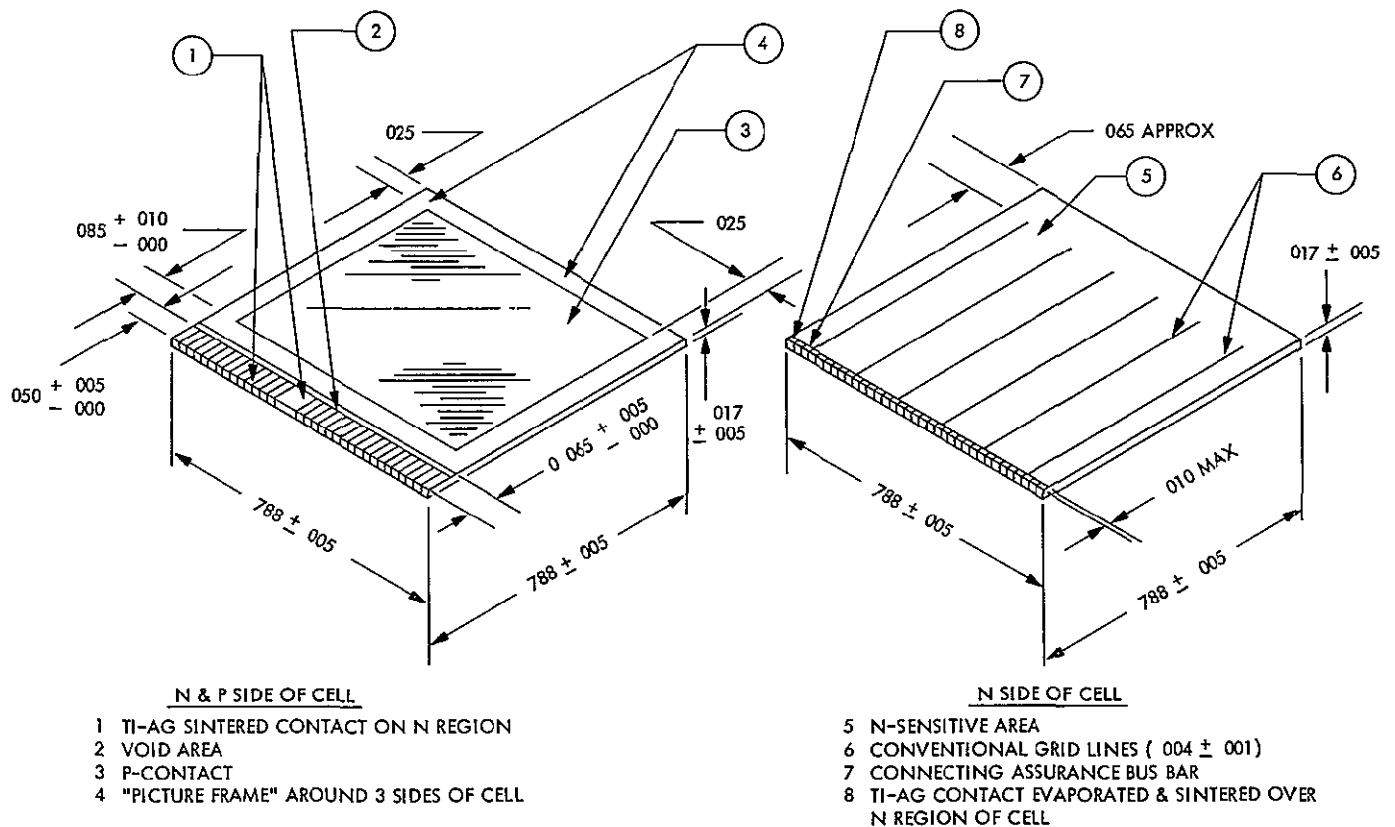


Fig. 3-3. Wraparound solar cell (Ref. 7)

The advantages expected of this construction technique are:

- 1) Lower cost (making subassemblies and panels)
- 2) More flexibility in achieving series parallel connections
- 3) The ability to use a single large optically coated cover glass over many cells
- 4) Large arrays (in many square feet) are possible in a single operation
- 5) More power for the same final size array
- 6) Flexibility of the module permits the fabrication of large deployable solar arrays.

Table 3-7. Wraparound modules -
Initial readings prior to thermal cycling (Ref. 7)

Module No.	I_{SC} ma	V_{OC}	I_{MP}	V_{MP}	Eff.	Power output, mw
140 mw						
AM = 0 equivalent						
10C	290	3.01	263	2.34	11.0	615
11C	294	2.99	263	2.32	10.9	610
12C	295	2.99	264	2.3	10.8	607
13C	302	3.01	267	2.32	11.1	619
14C	296	3.02	266	2.335	11.1	621
15C	299	3.02	268	2.34	11.2	627
16C	298	3.01	266	2.305	10.9	613
3S	290	3.00	256	2.335	10.7	598
4S	293	3.005	263	2.31	10.8	608
5S	286	3.01	256	2.335	10.7	598
Avg.	294.3	3.05	263.2	2.32	10.9	612
100 mw						
AM = 1 equivalent						
10C	243	2.985	220	2.35	12.9	517
11C	245	2.98	220	2.34	12.9	515
12C	247	2.98	218	2.335	12.7	509
13C	252	2.98	223	2.32	12.9	517
14C	248	2.995	222	2.34	13.0	519
15C	250	2.995	225	2.34	13.2	527
16C	249	2.99	222	2.335	13.0	518
3S	243	2.975	213	2.34	12.5	498
4S	244	2.98	223	2.31	12.9	515
5S	240	2.985	212	2.37	12.6	502
Avg.	246	2.985	220	2.34	12.9	514

Table 3-8. Wraparound Modules -
After 25 thermal cycles of -78.5°C to +60°C (Ref. 7)

Module No.	I _{SC} ma	V _{OC}	I _{MP}	V _{MP}	Eff.	Power output, mw
139.6 mw						
AM = 0 equivalent						
10C	291	3.01	262	2.325	10.9	609
11C	296	3.05	267	2.33	11.1	622
12C	298.5	3.01	268	2.30	11.0	616
13C	304.5	3.015	270	2.315	11.2	625
14C	299.5	3.015	268.5	2.325	11.1	624
15C	300	3.015	266	2.325	11.0	618
16C	300.5	3.015	264	2.315	10.9	611
3S	294	3.10	258	2.34	10.8	604
4S	296	3.10	266	2.30	10.9	612
5S	290	3.05	259	2.33	10.8	603
Avg.	297	3.04	265	2.32	11.0	614
100 mw						
AM = 1 equivalent						
10C	243	2.995	222.5	2.365	13.2	526
11C	246.5	2.99	221	2.35	13.0	519
12C	249.5	2.995	221	2.35	13.0	519
13C	253	2.995	225.5	2.335	13.2	527
14C	249.5	3.00	224	2.35	13.2	526
15C	251.5	3.00	225.5	2.35	13.2	530
16C	251	3.00	226.5	2.325	13.2	527
3S	244	2.995	215	2.35	12.6	505
4S	246	2.99	221.5	2.33	12.9	516
5S	241.5	2.995	216	2.345	12.7	507
Avg.	248	3.00	222	2.35	13.0	520

3.6 WRAPAROUND CELL FABRICATION

The evaluation of three processing techniques were included as part of the wraparound cell program. Two processes (Variations I and II) were identical except in the method of keeping the N/P junction from being shorted by the metallic contact material. Variation I provided a mask over the exposed junction (on the back of the cell) during evaporation of the contacts. Thus, no metal was deposited in this region. Variation II showed metal evaporated over the entire back. Then, with all other areas protected, the metal was etched off a small area extending the width of the cell and, consequently, separating the N and P contacts. Variation I was found to be most satisfactory from a fabrication point of view, and the cells for a module assembly were fabricated using this method.

A third variation was constructed using silicon dioxide as a diffusion mask. The SiO_2 was used to protect the desired P region on the back of the solar cell from being diffused. After diffusion of the N layer, the SiO_2 was removed and the contacts were evaporated in the same manner as Variation I. The aforementioned process should ultimately be used to construct the wrap-around cells. During this program, however, the growth of the SiO_2 at high temperatures (1100°C) caused a lowering of the lifetime in the P starting wafer. This resulted in a lower output than the cells of Variation I, and consequently, these cells were not used in the modularization. After the cell program had been completed, it was found that new methods for growing SiO_2 at low temperatures (200 to 300°C) had been developed. Future programs involving the wraparound techniques should re-evaluate the SiO_2 masking because it appears to have the ultimate lowest cost potential.

Current voltage characteristics of thirty cells, ten made with each processing variation, were measured at temperatures of -40 , 0 , 25 , 75 , 100 , and 125°C . The respective curves are shown in Figs. 3-4, 3-5, and 3-6.

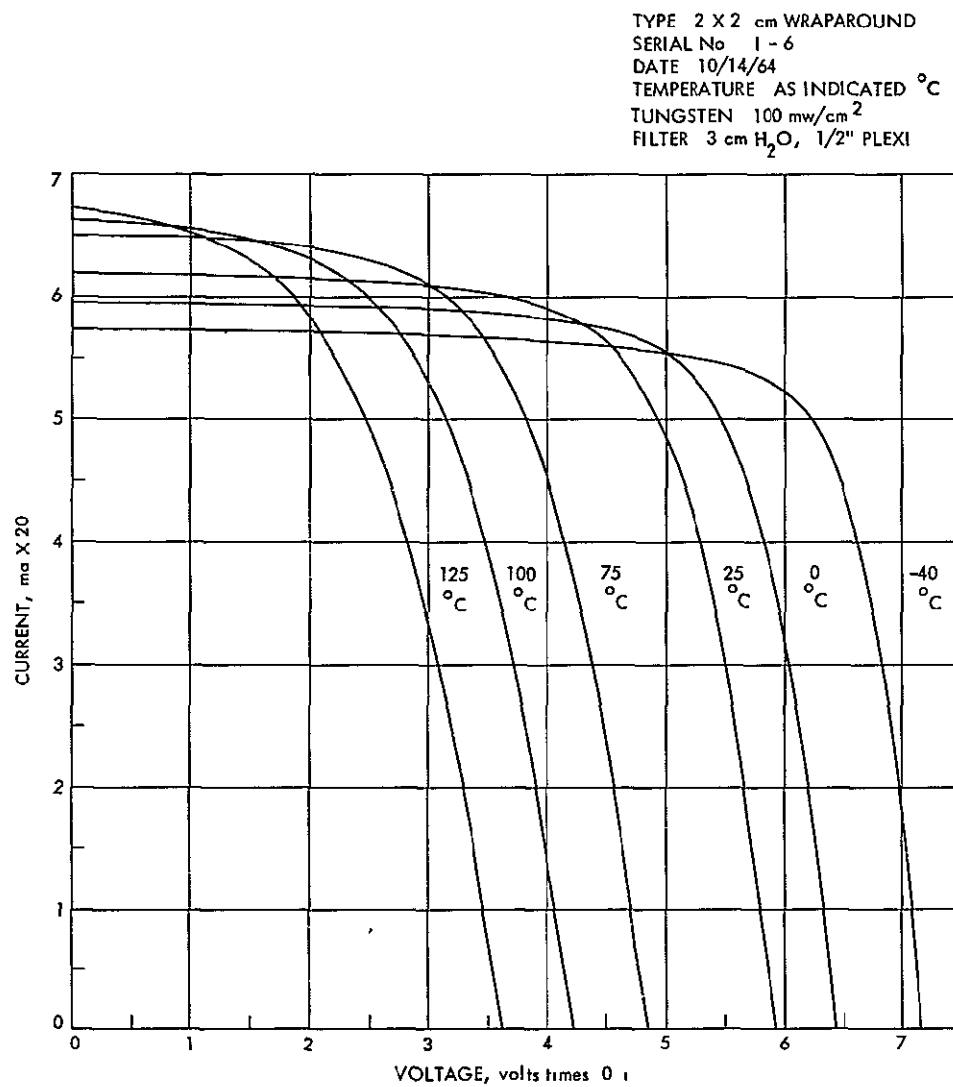


Fig. 3-4. RCA N/P silicon solar cell current-voltage characteristics (Ref. 7)

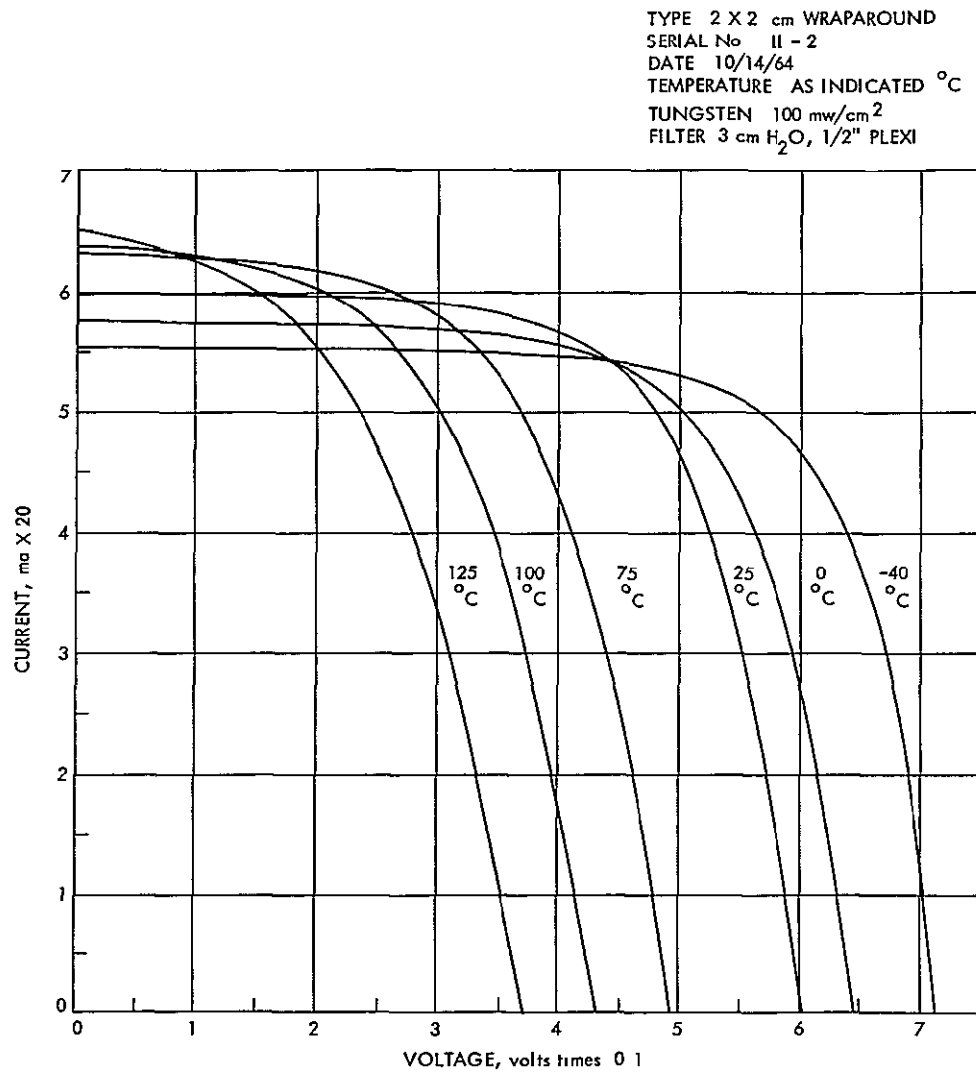


Fig. 3-5. RCA N/P silicon solar cell current-voltage characteristics (Ref. 7)

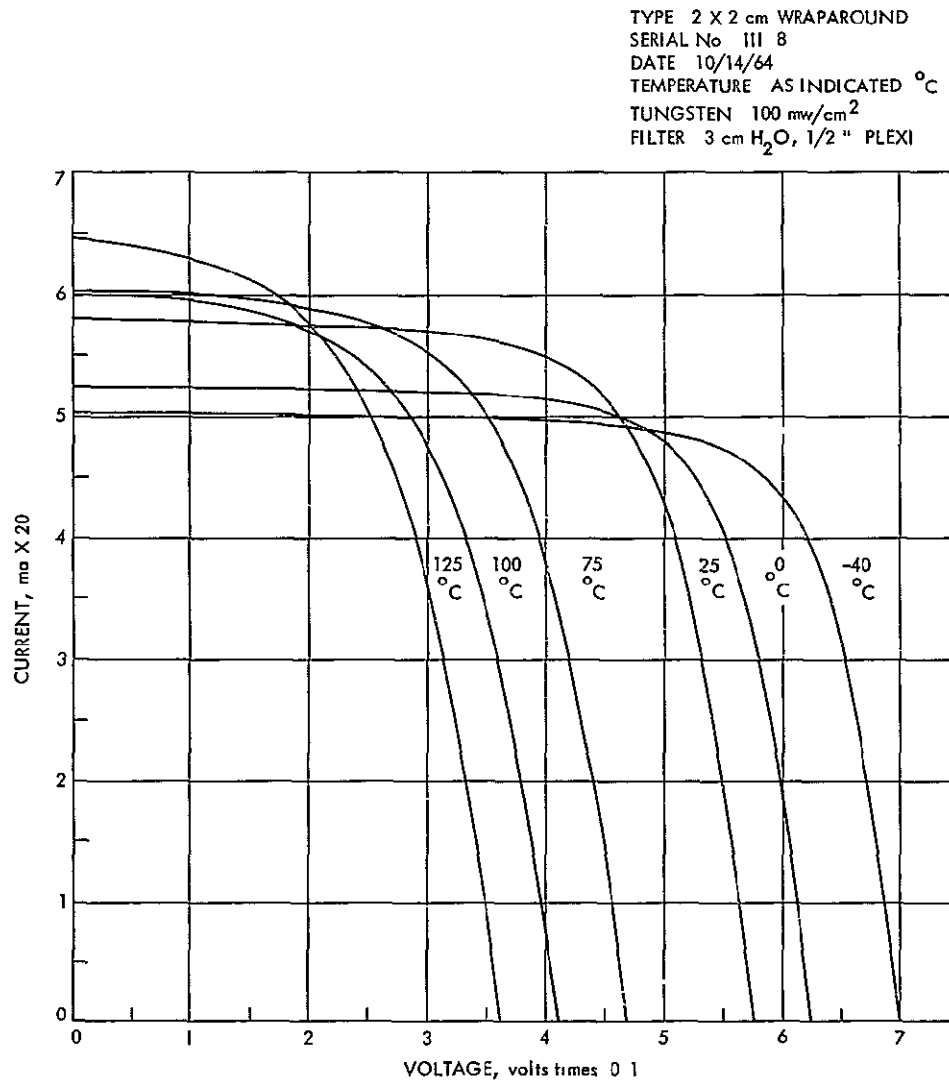


Fig. 3-6. RCA N/P silicon solar cell current-voltage characteristics (Ref. 7)

SECTION IV
MATERIALS

Summary

- 4.1 Solar Cell Adhesives
- 4.2 Dielectric Materials
- 4.3 Miscellaneous Material Systems

PRECEDING PAGE BLANK NOT FILMED.

SUMMARY

A variety of adhesives, dielectric materials, and miscellaneous material systems which have been used, tested, or considered for solar cells are reviewed. Some materials such as epoxy adhesives are considered unacceptable for solar cells because their bond strength is too high, i.e., they can not be easily removed for repair during fabrication.

SECTION IV

MATERIALS

4.1 SOLAR CELL ADHESIVES

Two adhesive system requirements exist in the solar cell area. One requirement is for an adhesive system to attach the solar cells to the structure, the second is to bond the solar cell cover glasses to the cells. The requirements for attaching the solar cells to the structure vary with the various arrays under consideration, but in general must have the following properties:

- 1) High thermal conductivity
- 2) Low outgassing in the vacuum environment
- 3) A modulus of elasticity compatible with the thermal motion of the cells and structure
- 4) Repairability during the fabrication phase (Ref. 8)
- 5) Must be relatively strong to resist vibration while at the same time able to absorb shock to prevent shattering of the solar cells
- 6) The adhesive must be a dielectric and provide electrical insulation between the solar cell and the panel structure to prevent a short-circuit (Ref. 9).

The adhesive for bonding the cover glasses to the solar cells must be transparent to electromagnetic radiation in the wavelengths from 0.4 to 1.1 microns (Ref. 8), and repairable in case the filter glasses are damaged during installation (Ref. 9).

4.1.1 Thermal Tests of Two Types of Adhesives for Bonding of Solar Cell Filter to the Cell

Two types of adhesives were selected for the test: Adhesive I, which was used for solar array assemblies and qualified by Hoffman Electromics in September 1960 for space applications, and Adhesive II, which shows promise

as a potential adhesive because of its ease of handling with a relatively short room temperature air-cure cycle and good optical transmission properties in the visible range. Before bonding, all filters were cleaned with isopropyl alcohol.

1) Adhesive I

Epocast 15E resin and Epocast 9010 hardener, mixed in a ratio of 2:1 parts by weight

Cure cycle: 8 hours at 200°F followed by 2 hours at 250°F

Manufacturer: Furane Plastics, Inc., Los Angeles, California

Method of Application: One drop applied to cell surface and spread over the entire interface area by pressing filter against cell.

2) Adhesive II

Epocast H-1368 resin and 9115 hardener (semi-rigid) mixed in a ratio of 1:22 PBW

Cure Cycle: Room temperature (75-80°F) for three hours

Manufacturer: Same as I above

Method of Application: Same as I above.

After data reduction, the electrical performance evaluation test with H-1368/9115 system shows a drop of more than 30% in power output, while the evaluation of 15E/9010 shows a drop in output varying from 0 to 3.9%.

The results computed in Table 4-1, together with sample inspection results, indicate that the H-1368/9115 adhesive system is not suitable for assemblies submitted to a high temperature environment (Ref. 9).

4.1.2 Tests of Adhesives for the Installation of Solar Cells on Photovoltaic Concentrating Panels

A number of commercially available silicone, polysulfide and epoxy materials were screened under the expected simulated environments of temperature and pressure. These results shown in Table 4-2 indicate the

Table 4-1. Comparison of V_{OC} , P/langley/min before and after thermal soak test (Ref. 9)

Sample No.		V_{OC}	ΔV_{OC} , %	I_{SC}	ΔI_{SC} , %	$\Delta \eta$, %
410-15E 3	before	0.568	-5.3	386	+1.8	64.7
	after	0.537		393		64.7 0
410-15E 4	before	0.565	+0.5	367	+0.5	65.0
	after	0.568		369		62.5 -3.9
410-15E 13	before	0.567	-0.5	378	+0.8	59.5
	after	0.564		381		58.2 -2.2
410 H-1368 12	before	0.564	-4.8	338	-10.3	63.1
	after	0.537		307		43.5 -31.1

V_{OC} refers to 28°C.

I_{SC} reduced for radiation values of 1.5 langley/min

P normalized to 28°C and for langley/min

All values are averages of three measurements

degrading effects that could be expected if the adhesives were outside Earth's atmosphere. Since sublimation or outgassing products of the adhesives used on the solar panel could redeposit on the solar cell or reflector surfaces and reduce the electrical efficiency, the percent weight loss after exposure would provide one parameter to determine the suitability of a material. In addition to these sublimation or outgassing tendencies, the adhesive must also withstand mechanical loads. Therefore, comparative tensile strengths of the applicable adhesives were determined after exposure to the combined effects of temperature and pressure. See Table 4-3. These results indicated

Table 4-2a Weight loss after exposure to pressures of 5×10^{-6} to 5×10^{-7} torr and temperatures of 200°F to 250°F for 100 to 112 hours (Ref. 10)

Material	Weight before exposure, grams	Weight after exposure, grams	Weight loss, grams	Weight loss, %	Observations
Flexible filled epoxy	26.557	26.290	0.267	1.01	No color change. Slight slump at bottom of sample.
Flexible silicone	15.928	15.808	0.120	0.75	No color or dimensional changes.
One component silicone sealant	3.936	3.734	0.202	5.13	No color or measurable dimensional change.
Clear flexible silicone	13.400	10.098	3.302	24.64	Slight darkening and loss of 1.5 mm from the surfaces of the 1" cube.
Modified dimethyl silicone	25.057	24.875	0.182	0.73	No color or measurable dimensional change
Phenolic rubber	4.3686	4.2668	0.1018	2.3	No color or measurable dimensional change
Epoxy polyamide	23.282	23.280	0.002	0.01	Slight darkening, but no measurable dimensional changes.
Polysulfide with chromate cure	14.610	13.641	0.969	6.63	Slight darkening. Sample bubbled and slightly expanded.

Table 4-2b. Weight loss after exposure to pressures of 5×10^{-6} to 5×10^{-7} torr and temperatures of 200°F to 250°F for 100 to 112 hours (Ref 10)

Material	Weight before exposure, grams	Weight after exposure, grams	Weight loss, grams	Weight loss, %	Observations
Epoxy with anhydride curing agent	11.552	11.535	0.017	0.15	Slight darkening, but no dimensional changes.
Epoxy with amine hardener	9.937	9.719	0.218	2.2	No color or dimensional changes.
Epoxy with versamid hardener	8.964	8.646	0.318	3.5	No color or dimensional changes.
Flexible epoxy with versamid hardener	9.156	8.962	0.194	2.1	Both surfaces frosted. No dimensional changes.
Polysulfide with lead oxide cure	15.617	10.354	5.263	33.70	Slight darkening. Sample bubbled and shrank approx. 25%.
Dimethyl silicone	16.237	16.105	0.132	0.81	No color or dimensional changes.

Table 4-3. Comparative tensile strengths of adhesive bonded aluminum specimens (Ref. 10)

Adhesive materials	Exposure conditions	Tensile average of 5 tests, psi
Mylar tape with polyester adhesive on both sides	Control	66
	Tenney Chamber	304
Epoxy polyamide	Control	184
	Tenney Chamber	773
Epoxy with an amine hardener	Control	36
	Tenney Chamber	155
Modified dimethyl silicone	Control	204
	Tenney Chamber	212
Methylphenyl silicone	Control	215
	Tenney Chamber	198
Dimethyl silicone	Control	157
	Tenney Chamber	154
One component silicone sealant	Control	7.5
	Tenney Chamber	12.9
Glass tape with phenolic rubber, thermal setting, adhesive on one side	Control	178
	Tenney Chamber	150
Dimethyl silicone with stannous octoate catalyst	Control	61
	Tenney Chamber	58
Phenolic rubber adhesive on a paper carrier	Control	49
	Tenney Chamber	50
Mylar tape with rubber adhesive on both sides	Control	50
	Tenney Chamber	48
Polyester film with phenolic rubber adhesive on both sides	Control	66
	Tenney Chamber	77
Fiberglass with silicone adhesive on both sides	Control	13
	Tenney Chamber	24
Fiberglass with modified epoxy adhesive on both sides	Control	230
	Tenney Chamber	417
Fiberglass with epoxy adhesive on both sides	Control	511
	Tenney Chamber	510

Tenney Chamber: pressures of 5×10^{-6} to 1×10^{-8} torr, and temperatures of 200°F to 250°F for 100 to 110 hours.

a wide variance in the lap-shear tensile strengths of the candidate adhesives (Ref. 10).

4.1.3 Epoxy-Polyamide Adhesives

The epoxy-polyamide adhesives have been used on the IMP spacecraft (FM-1000) and on the Mariner 1964 solar panels. Their performance in space has apparently been satisfactory. The structural loads developed in the array during launch are direct functions of the structural damping provided by the adhesive system used in fabrication of the bonded beryllium frame members. Several polymeric systems were considered. Most systems exhibited little energy absorbing capability or had not been space-qualified. The epoxy-polyamide adhesive "BMS 5-29" exhibits desirable structural damping characteristics and was, therefore, selected as the structural bonding agent (Ref. 8).

It should be noted that some epoxies have poor shock absorbing characteristics with the resultant possible shattering of the solar cells (Ref. 10).

4.1.4 Other Adhesives Used

Table 4-4 is a partial list of adhesives used to bond the cover glass to the cell and to bond the cell to the substrate. Tables 4-4 and 4-5 are a partial list of the adhesive properties. Table 4-6 is a partial list of conductive adhesives. Other conductive adhesives not listed, but reported as used, are GE SMRD 745 Flexible Epoxy (the same mixed 50-50 with Ag) and Epoxy Products EP 3026.

4.2 DIELECTRIC MATERIALS

Dielectric materials are used to isolate electrically the solar cell and its interconnect system from the substrate while providing other functions such as an adhesive to hold the solar cell to the substrate.

Table 4-4. Properties of cover glass adhesives (Task 15)

Property	Material				
	RTV-602	RTV-615	Sylgard 182	Sylgard 184	Dow Corning 93-500
Color	Colorless	Lt. straw	Lt. straw	Lt. straw	Colorless to Lt. straw
Specific gravity	0.995	1.02	1.05	1.08	1.08
Durometer, hardness, Shore A	15	35	40	40	
Viscosity (poises)	0.8 - 1.5	3.5	55	55	80
Thermal conductivity (Cal. 1 cm 1°C/sec)			5×10^{-4}	3.5×10^{-4}	3.5×10^{-4}
Coef. of expansion (-in. 1 in. 1°C)			300	300	300
Refractive index	1.406	1.406	1.430	1.430	
Tensile bond strength (psi)		800 - 1000	800	600	790
Volume resistivity (ohm-cm)	10^{14} 14 hr @ 25	10^{14} 24 hr @ 150°C	2×10^{15}	6.9×10^{13} 4 hr @ 65°C	6.9×10^{13} 24 hr @ 125°C
Volatile condensables					
Wt. loss, %	3.10	1.01		1.77	
VCM wt., %	0.96	0.77		0.89	

Table 4-5. Properties of solar panel adhesives and primers (Task 15)

	Adhesives		Primers		
Property	RTV -40	RTV -41	SS -4044	Dow-Corning 1200	SS -4004
Specific gravity	1.35	1.31	0.85		0.85
Viscosity (poises) @ temperature	300 - 600	350 - 500		0.01	
Durometer, hardness (Shore A)	55	50			
Tensile strength (psi)	550	500			
Elongation (%)	120	200			
Color	white 24 hr @ 75°C+ 24 hr @ 275°C	white	clear 24 hr @ 150°C	red	flourescent pink 24 hr @ 150°C
Volatile condensables					
wt loss %	1.07		1.05		0.40
VCM wt. %	0.56		0.35		0.20

Table 4-6. Properties of conductive adhesives (Task 15)

Property	Material				
	Eccobond solder 56C	Eccobond solder 57C	Eccobond solder 58C	Eccobond solder 70C	Eccobond solder V-91
Temperature range of use, °F	-70 to +350	-70 to +350	-65 to +500	-70 to +300	-50 to +300
Bond shear strength, psi	450	500	1600	1000	500
Flexural strength, psi	12,200	10,200	9700		
Volume Resistivity, ohm/cm	$<2 \times 10^{-4}$	$<6 \times 10^{-4}$	$<2 \times 10^{-3}$	$<2 \times 10^{-3}$	$<2 \times 10^{-3}$
Thermal conductivity, btv/sq ft/in. /°F/ht	>200 16 hr @ 50°C	>200 16 hr @ 52°C	>200	>200	
Volatile condensable materials					
wt. loss %	0.30	0.67			
VCM wt. %	0.30	0.06			

4.2.1 Mariner-Venus 1967

Seven different candidate dielectric material test specimens were evaluated for possible use on the MV 1967 solar panels. The results of this test program have been summarized in Table 4-7 (Ref. 11).

Of the parameters evaluated, discoloration was considered least important in the selection of dielectric materials. Table 4-7 shows that although all specimens apparently passed the insulation resistance test, which is most important for a dielectric material, each exhibited some defect in one or more of the other parameters considered.

Delamination is a failure mode which cannot be tolerated for any material used on the spacecraft. Thus, the Ranger dielectric (epoxy board and RTV-40) was disqualified.

Material flow and penetration are directly related to material properties and are evidence of chemical or mechanical change. Thus, the materials exhibiting these characteristics (SMP 62, 63, and PT-410) after short test periods could not be expected to survive a long term mission under the conditions predicted for MV 1967 spacecraft.

Epon 956 was the only material to pass all critical tests, with the one exception of electrical leakage during wet resistance testing. Normally, any material failing this test should be disqualified from use, however, in this case several factors were considered.

- 1) Each of the other dielectric materials, except the Ranger type, were applied in three separate 1-mil layers. This technique normally eliminates leakage paths.
- 2) At the time the application technique for this material was derived, the problem of leakage was not considered serious by the materials and structures personnel at JPL, thus, only one layer of dielectric was considered necessary (especially with a positive 2-mil glass cloth layer). Most liquid coating materials can be expected to allow leakage paths when applied in a single coat.

Table 4-7. Test results summary (Ref. 11)

Material Parameter	SMP 62, 63 MC -64	SMP 62, 63 New	SMP 62, 63 with white pigment	PT -401	3-mil epoxy/ glass cloth with RTV -40	Epon 956	Epon 956 with 2-mil glass cloth
>100 megohms insulation resistance	P	P	P	P	P	P	P
Delamination	P	P	P	F	P	P	P
Electrical leakage path to substrate	P	P	P	P	P	F	F
Flow	F	F	F	F	P	P	P
Discoloration	F	F	F	F	F	F	F
Penetration of weighted small (0.005 in. dia.) objects	F	F	F	F	P	P	P

P = Passed

F = Failed

- 3) Initially, the material was applied by brush and had a xylene thinner. This was later found to be undesirable due to chemical incompatibility of the xylene with epoxy. (MEK and acetone were adopted as replacement solvents, and spray coating was adopted in place of the manual brushing technique.)
- 4) Table 4-7 verifies that the common, dry insulation resistance test was passed. The dielectric failed only when a wet resistance test was experienced. The wet test heretofore was not a test parameter.

Based on these tests and the results experienced, it can be tentatively concluded that of the materials evaluated, only Epon 956 with glass cloth is worthy of further consideration at this time.

These tests were directed towards the establishment of one to several dielectric materials suitable for use on the MV 1967 solar panels. It was felt that any of the materials considered could be used if required, these tests merely served to establish a level of confidence for each of them. This being the case, the test environments were made much more severe than predicted for the mission in an attempt to.

- 1) Disqualify marginal materials, this goal was accomplished.
- 2) Determine design limits or ability to withstand mission perihelion environments, this goal was tentatively accomplished and further investigation and changes in application techniques are warranted. (Ref. 11)

4.2.2 LEC Laboratory

LEC Solar Research and Development Laboratory developed an engineering model to test the design of a flexible solar cell interconnect system.

The substrate was insulated with EPON 956 epoxy resin (Shell Chemical Co.) and Style 108 glass cloth (J.P. Stevens). The insulation thickness as bonded is 3 mils. Insulation was bonded during structure fabrication by Ryan Astronautical Co.

The solar cell module assemblies are bonded to the honeycomb substrate with GE 577, RTV material. Cover slides are bonded to cells with DOW XR -6-3489 transparent silicone rubber material.

4.3 MISCELLANEOUS MATERIAL SYSTEMS

In efforts to improve solar cells, many material systems may be considered. Some of these material systems have previously been investigated for use in silicon transistors. The more subtle disadvantages are just beginning to become apparent. As an example, aluminum is still the material most commonly used as interconnection metal in transistors. It is now known to have limitations of: (1) reacting with gold, (2) migrating at elevated temperatures and high current densities, (3) attacking silicon dioxide, and (4) forming gross grain structure which increases the resistance.

Three systems are presented for information purposes.

4.3.1 Titanium-Gold

The titanium-gold system has shown some promise in the high current density tests, where conductor strips on SiO_2 are subjected to high currents and elevated temperatures for many thousands of hours.

In most of the tests of the titanium-gold system, the titanium film was limited to 1000 \AA , it was found that increasing the thickness of the titanium increased the resistivity of the metallization, and greatly accelerated the thermally induced resistance rise. The resistivity of 2000 \AA of titanium and 2000 \AA of gold increases by a factor of 15 times in 15 min at 450°C . With 500 \AA of titanium, alloying of gold with exposed silicon occurs in less than 15 min at 450°C . In tests at 300°C , alloying of the gold with the silicon occurred in about 1 hr. These alloying tests were performed in dry air, dry nitrogen, and also a vacuum environment. Where the titanium-gold metallization is in contact with $10,000 \text{ \AA}$ of thermal SiO_2 , the physical deterioration started in ≤ 15 min of 450°C , but showed little or no deterioration at 300°C after 16 hours. The deterioration has also been observed under a passivating glass layer.

SECTION V
INTERCONNECTS

Summary

- 5.1 Introduction
- 5.2 Intercell Connections
- 5.3 Interconnect Design
- 5.4 Designing Out Stresses
- 5.5 Interconnect Materials

Thus, it is apparent that, similar to the chromium-gold-system, alloying of the gold with exposed silicon is the limitation of the titanium-gold metallization system.

4.3.2 Titanium-Platinum-Gold

Films have been prepared by sputtering titanium ($\sim 1500\text{\AA}$) layers on oxidized silicon wafers. The films were etched to form the desired test pattern, then $\sim 5000\text{\AA}$ of gold was deposited by vacuum evaporation or electrodeposition. Sputter etching of the three-layer metallization was also used to produce patterned wafers.

Thermal tests at 300 and 450°C in air have shown that the resistance of the titanium-platinum-gold system increases significantly with time. The initial resistivity of the films was between 4 and 6 microhm-cm. The highest increases are associated with gold films $\leq 5000\text{\AA}$ thick.

The three-layer metallization using the platinum layer was very effective in preventing alloying of the gold with exposed silicon. Overnight tests at 450°C showed no alloying. The thermally induced resistance increases limit this system for long term high temperature processing. Recent results indicate that this resistance rise can be limited by control of the film thicknesses. By optimizing the thickness of the titanium, platinum, and gold, this system may be desirable for special applications (Ref. 12).

A more recent report from Bell Laboratories describes "micro-bridges" which are integrated circuit leads which cross others through the air, without touching the lead below. The metals systems involved in this technique are titanium-platinum-gold. In the "microbridge" technique, thickness determination of the metal films and possible interaction of the metals at elevated temperatures are critical (Ref. 13).

4.3.3 Gold-Silicon System

The Au-Si film combination is similar to the gold-tantalum system in several respects. Initial adhesion is good, while lifting occurs after some time in room air although the time period is somewhat longer than in the Au-Ta case. Furthermore, the adhesion of Au to oxidized Si is as poor as to

Ta_2O_5 . Drastic differences between the two systems occur upon heating to 270°C in air. After this treatment, the adhesion at the Au-Si interface is improved to such an extent that no separation takes place there, but may occur at the Si-glass interface. The latter effect depends on the thickness ratio R . For $R < 0.8$, the film combination remained adherent to the glass for 70 days (end of test period) while for larger values of R , partial and - eventually - complete lifting was observed as a function of time. This effect was independent of the environment. Heat treatment at higher temperatures only accelerated the process, i.e., reduced the time of adhesion (Ref. 14).

SUMMARY

The design and geometry of interconnects are reviewed from the early rigid shingle design to the present expanded mesh approach. The selection of materials and their associated coatings are discussed, including considerations for processes used to make the electrical connections. The present trend appears to be toward extensive use of expanded silver mesh.

PRECEDING PAGE BLANK NOT FILMED.

SECTION V

INTERCONNECTS

5.1 INTRODUCTION

The use of interconnections in the solar cell arrays, though appearing simple, is indeed a fairly critical area and merits careful consideration. There are various aspects ranging from intercell connections to interpanel connections. Problems associated with these areas are often underestimated as evidenced by the numerous difficulties which have been encountered with some solar cells, methods of construction, and process techniques. This particularly relates to intercell connections within groups of cells in an unbroken interconnected series-parallel arrangement.

5.2 INTERCELL CONNECTIONS

Electrical power for spacecraft systems is generally provided by large numbers of solar cells connected in both series and parallel to obtain the required voltages and currents. Until the end of 1960, most solar cell arrays were arrangements of series connected modules, each consisting of a small number of cells connected in series, generally about five cells. These five-cell modules were assembled by soldering the front contact strip of each cell to the bottom of the opposite side of the adjacent cell, forming a "shingle" as shown in Fig. 5-1. With the conventional shingle arrangement, a rigid structure of about 2 x 4.6 cm (for five cells) is formed by crystalline silicon cells soldered together.

The geometry of this configuration creates high stress points, especially at the intercell contacts. Such assemblies have led to frequent problems, in many cases as the result of aging from repetitive thermal cycling. In one investigation, a loss in current of 75% was shown to occur for a rigid shingle assembly due to very small distortions in the substrate caused by thermal cycling. For a similar bank of cells on the same panel, assembled with the Spectrolab Solaflex System, not one cell was lost (Ref. 17).

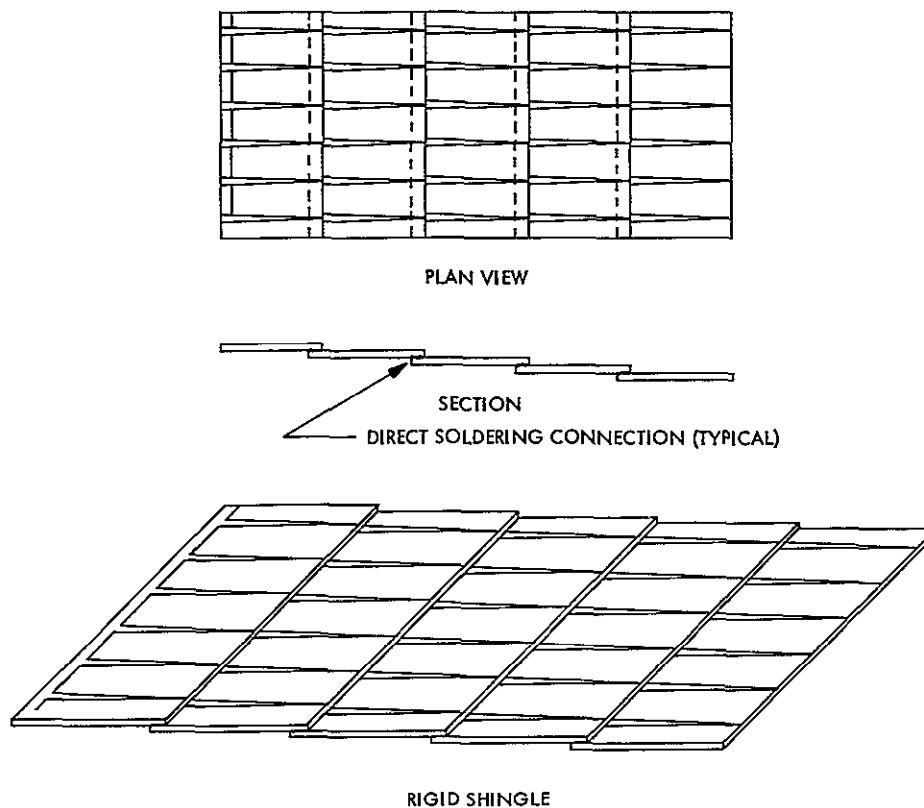


Fig. 5-1. Rigid shingle (Ref. 17)

Recognizing the problem arising from the significant thermal and mechanical stresses within such rigid assemblies, Spectrolab introduced the "Solaflex" system of interconnection at the beginning of 1961. The Solaflex technique is based upon the use of parallel bused submodules. In this arrangement cells are connected into small parallel groups, using a "tab strip" soldered along the bottom of the cells. The series interconnecting tabs extend out and up from the edge of the bus, and are stress relieved before connection with the next succeeding series group, as shown in Fig. 5-2 for an early version of the design. Considerable redundancy is achieved by use of these multiple tabs and connections.

Upon mounting, each cell is independently suspended on its own resilient adhesive pad, isolated from the other cells except for electrical contact through flexible, stress relieved tabs. Thus, virtually no forces are transmitted from cell to cell. As a result, thermal stresses are minimized,

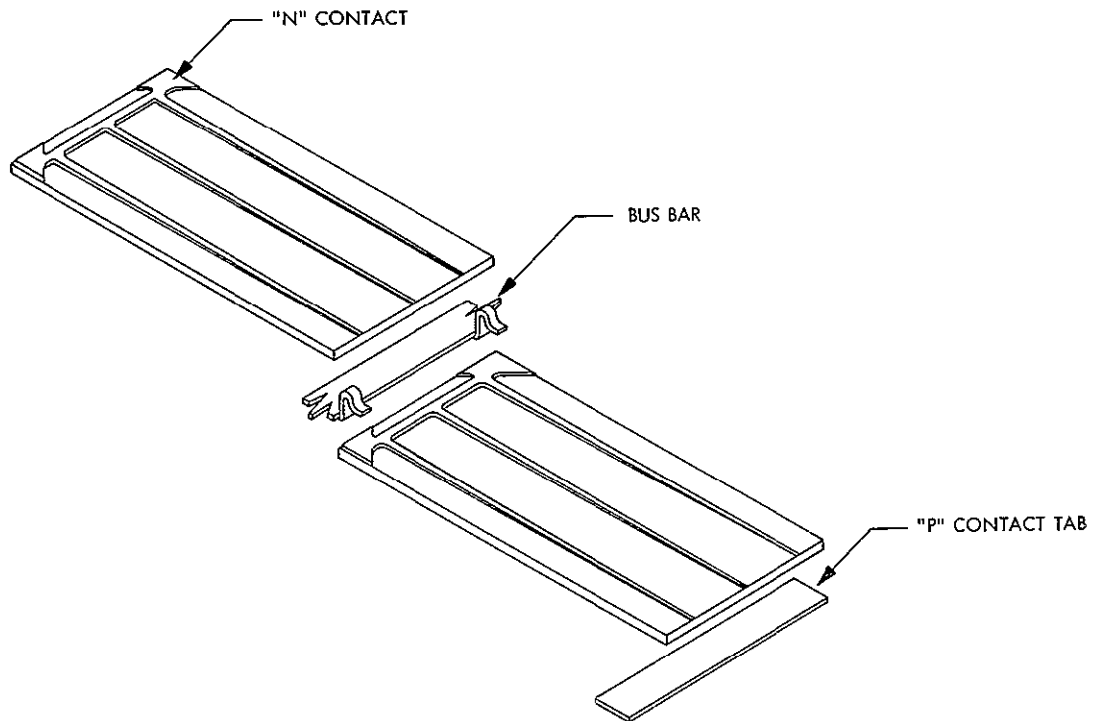


Fig. 5-2. New interconnect approach (Ref. 17)

and since the array is more flexible, it is less likely to fail due to vibration or shock environments (Ref. 17).

Another feature of this cell interconnection system is that parallel current loops are effectively eliminated, that is, in a circuit using matched cells, current flow is in the series direction only, parallel flow being eliminated. In the case of mismatch or cell degradation, only the differential current is distributed in the parallel direction.

Even in the case of individual cell failure or degradation, this interconnection system substantially increases reliability. The same parallel contact strip connects all adjacent series units with at least two connections (in some cases four) per cell (for a 2 x 2 cm cell). Moreover, parallel interconnections made across both the N- and P- sides of parallel adjacent cells provide redundancy in both parallel and series directions. The spacing between the cells in series can be reduced to a nominal 17 and 10 mils in parallel, thus giving excellent area utilization.

To further reduce the possibility of interconnection failure, the Solaflex interconnection technique now incorporates a bus bar with extended interconnectors or tabs on the underside of the cell, so as to locate the positive and negative connections in close proximity on opposite faces of the cell. Illustrations of this extended bus system are shown in Figs. 5-3 and 5-4.

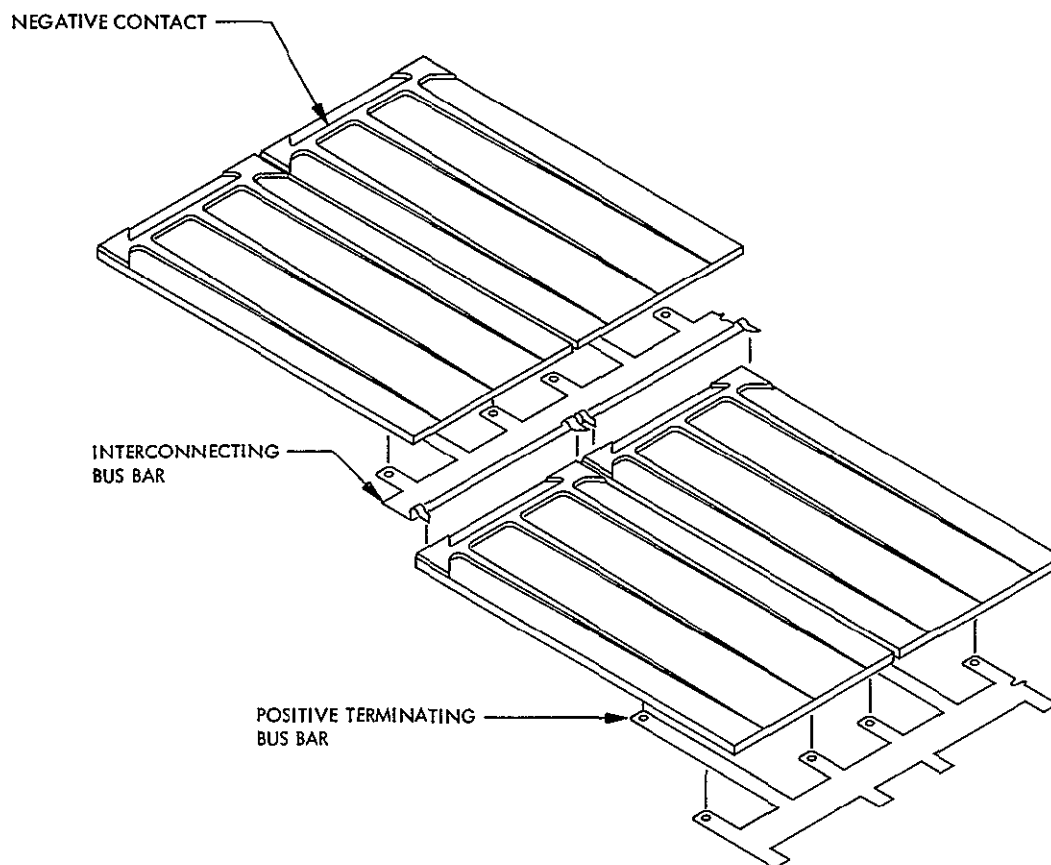


Fig. 5-3. Solaflex series parallel arrangement using type AT-2010 cells (Ref. 17)

The use of the series parallel planar arrangement of solar cells described in Figs. 5-3 and 5-4, and developed by Spectrolab, are covered by U.S. Patent No. 3094439, now reissued as Patent No. RE 25,647 assigned to ¹ Spectrolab, Division of Textron, Inc., and by additional pending patents.

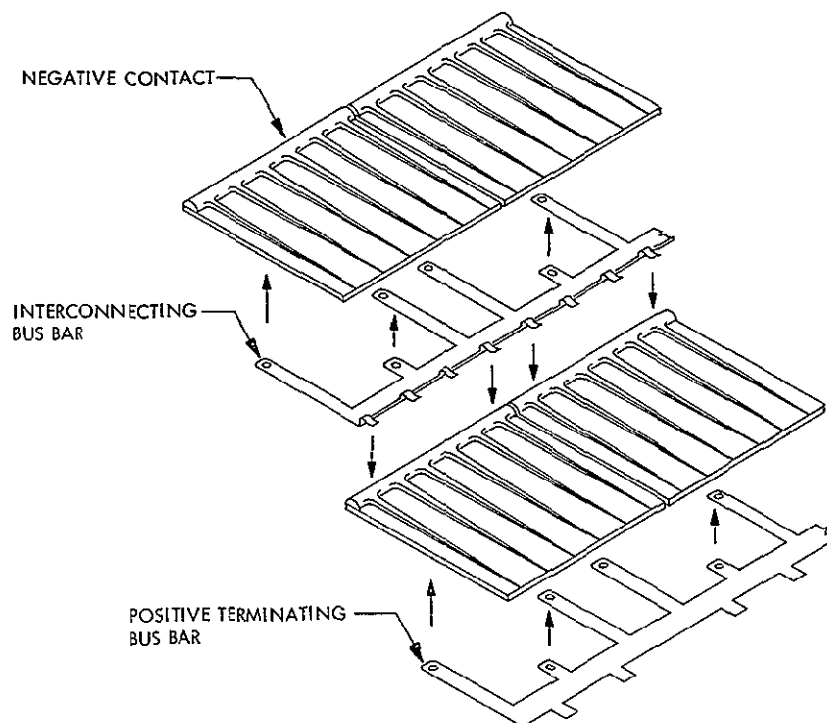


Fig. 5-4. Solaflex interconnections using type AB-2020 cells (Ref. 17)

Two additional Spectrolab configurations are illustrated in Figs. 5-5 and 5-6. Figure 5-5 illustrates the specified 2 x 2 cm cells interconnected as

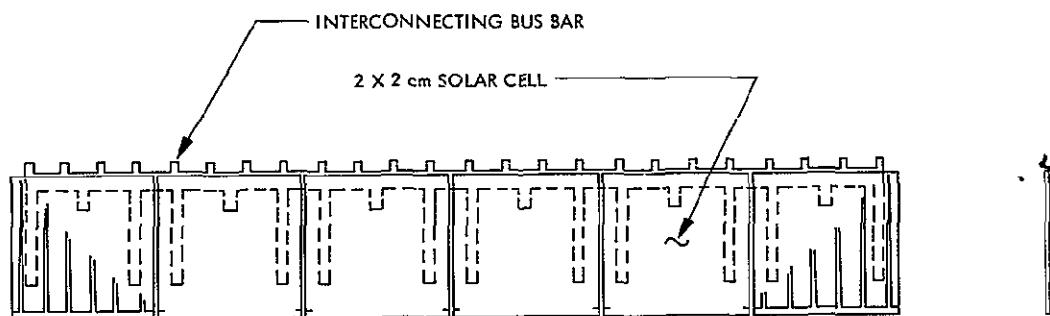


Fig. 5-5. Submodule 2 x 2 cm cells x 6 cells wide (Ref. 17)

described above, and Fig. 5-6 illustrates the interconnection of the large area 2 x 6 and 2 x 7.15 cm cells (Ref. 17).

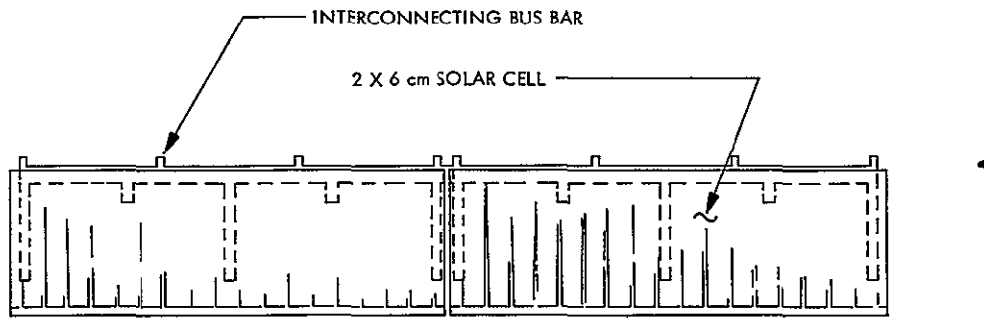
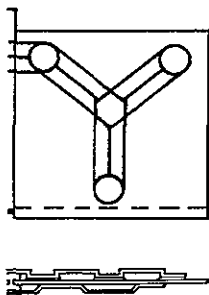


Fig. 5-6. Submodule 2 x 6 cm cells x 2 cells wide (Ref. 17)

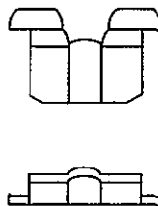
5.3 INTERCONNECT DESIGNS

Many companies have been very active in this area. In fact, it can be assumed that every company involved in designing solar cell packages has its own "pet" design(s) which it considers proprietary. Figures 5-7(a) through (f) illustrates the variety in design.

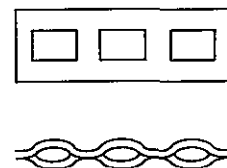
Many designs now utilize mesh screen wire under various names (see Fig. 5-7(f)). The major differences being the materials selected, the method of manufacture, and the size of the mesh.



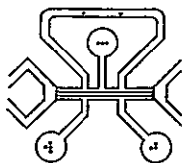
(a) LOCKHEED



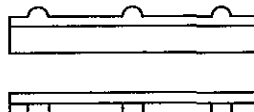
(b) TRW



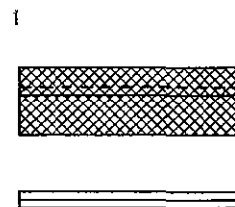
(c) TRW



(d) JPL



(e) Industry-wide



(f) Industry-wide

Fig. 5-7. Interconnect configuration varieties

All of these designs attempt to provide the ultimate in connecting a number of cells (generally 5 or 6) together for a parallel group and at the same time connect to another identical group in series. All provide a redundancy in electrical connections with some designs actually intended to operate under the conditions of a partial cell or a complete cell failure.

Processes also may establish the material requirements. Example: The use of welding as an interconnect process requires materials that can be welded. A number of different materials can be used for the weldable bus bars. The assembly technique is the same regardless of material. However, a compromise between ease of welding, electrical conductivity, and compatibility between the cell and bus bar material is necessary.

Three typical materials available for selection are compared.

- 1) Dead soft copper, tin plated
- 2) Nickel "A"
- 3) Kovar

Either of these can be used. However, copper has the best electrical conductivity, nickel is the most easily welded, and Kovar provides the best match with silicon in coefficient of thermal expansion. The final selection will depend upon what interconnect requirements are considered most important.

One design for welding uses a P bus bar, Fig. 5-8, and an N bus bar, Fig. 5-9. The final configuration is shown in Fig. 5-10.

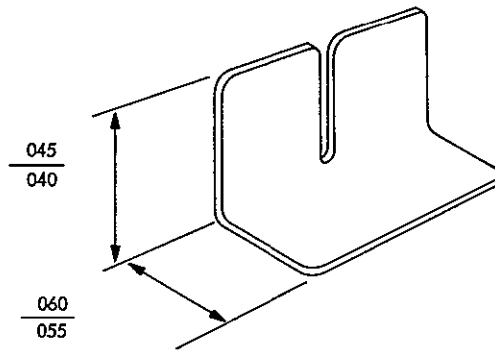


Fig. 5-8. 'P' Tab 612742 - after forming (Ref. 18)

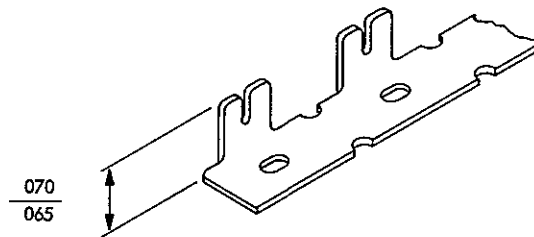


Fig. 5-9. 'N' Bus bar 612738 - after forming (Ref. 18)

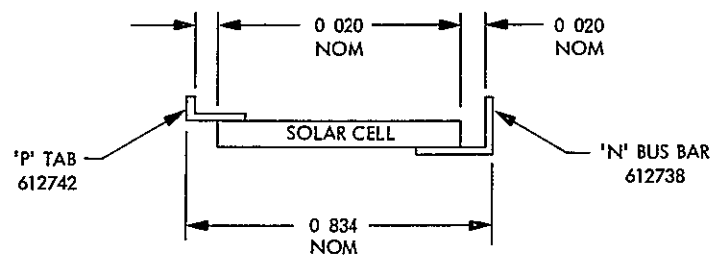


Fig. 5-10. Submodule subassembly - before welding (Ref. 18)

5.4 DESIGNING OUT STRESSES

There is considerable concern about the stresses involved when soldering a metal to a glass. These stresses are caused by the difference in thermal expansion and conduction of the materials involved, the soldering (or other) processes involved, and the interconnect forming techniques. If these stresses are allowed to accumulate at one point and exceed the material/joint capabilities, failure will occur.

One approach to interconnect design is to avoid connecting adjacent solder joints by a straight section of interconnect. The theory behind this approach is that the stresses imposed at one solder joint should not be allowed to travel a straight line to the adjacent solder joint.

5.5 INTERCONNECT MATERIALS

The materials used for interconnects include, but are not limited to, copper and its alloys, aluminum, nickel, silver, gold, Kovar, and molybdenum. Typical coatings are silver, gold, tin, or solder.

The selection of a material and its coating (if used) is established by the environment that the cell will be exposed to, and how high the stresses are determined to be between the cell and the interconnect. Generally, the designer trades off between the thermal properties (between cell and interconnect) and the electrical properties (Table 5-1) keeping in mind the interconnect process to be used.

There is no simple formula for the selection of the interconnect material or its coating. A mission requirement for non-magnetic materials would eliminate Kovar. Copper or silver could be used. Silver (maybe a mesh design) would eliminate the need for a plating. Copper, on the other hand, is not as expensive and more available so that economics may dictate such a choice.

A list of materials and coatings were compiled in Table 5-2 from verbal discussions with numerous companies.

Table 5-1. Physical and mechanical properties of metals used in solar cells (Task 15)

Property	Metal										
	Al	Ti	Ni	Cu	Mo	Pb	Ag	Sn	Au	Kovar ^a	Si
Density (lb/in ³)	0.098	0 163	0 322	0 324	0.369	0 41	0 379	0.208	0 698	0 302	0 084
Coef. thermal expansion (-in/in°C)	23 0	4 67	13.3	16 5	4 90	29 0	17.0	23.0	14 2	5 0	3 0
Thermal conductivity (cal/sq cum/cm/°C/sec)	0.57	6.6	0.22	0.941	0 34	0.083	1 0	0 15	0 71	0 40	0 20
Electrical conductivity (% IACS)	64.9		25	103	34	8 3	106	15.6	73 4		
Electrical resistivity (-ohm cm)	2.65	42	6.84	1.67	5 2	20.6	1 59	11 0	2 19	49	10.00
Magnetic susceptibility (10 ⁻⁶ cgs)	0.6	-3 17		-0 08	-0 93	-0 01	-0 02	-0 03	-0 15		-0 13
Modulus of elasticity (10 ⁶ psi)	9 0	16 8	30	16	47	2	11	6	11	30	16.35
Specific stiffness (E/P x 10 ⁶ in)	92 0	103	93	49.4	127	4.9	29	28 9	15.8	99.3	195.00
Tensile strength (10 ³ psi)	6 8	34	46			1.9	18 2		19	77 5	
Yield strength (10 ³ psi)	1.7	20	8 5			0 8	7 9		40	59 5	
Elongation (%)	60	54	30			30	50			16 8	

^aKovar is not a pure metal, but rather an alloy of the following composition 29 Ni, 17 Co, 53 Fe

Table 5-2. Materials and coatings used in interconnects
(verbal contact source)

Material	Coating	Process ^b
Aluminum		U, T
Be-Cu	W/WO ^a Tin	I
Cu	W/WO ^a Tin, Silver	O, I
Gold		H, U, T
Kovar	Tin, Gold, Silver	I, R, M
Mo	Gold	H
Ni		W
Silver		I, P, T, N
Platinum		U
Silver-Tin Alloy		U
^a W/WO = With and without ^b Processes <div> <div>U = Ultrasonic bonding</div> <div>O = Tunnel oven</div> <div>R = Reflow soldering</div> <div>P = Hand soldering</div> <div>T = Thermal compression bonding</div> <div>H = Heated bar</div> <div>M = Induction heating</div> <div>N = Oil solder bath</div> <div>I = Infrared heating</div> <div>W = Welding</div> </div>		

SECTION VI
INTERCONNECT PROCESSES AND SOLDERING MATERIALS

Summary

- 6.1 Introduction
- 6.2 Reflow Soldering
- 6.3 Tunnel Ovens
- 6.4 Resistance Welding
- 6.5 Ultrasonic Bonding
- 6.6 Infrared Heating
- 6.7 Induction Heating
- 6.8 Other Soldering Approaches
- 6.9 Comparison of Soldering Methods
- 6.10 Soldering Materials

SUMMARY

The soldering process has been used most extensively to make the electrical connection (joint) between the interconnect and the solar cell(s). The process has undergone considerable refinement and advancement from the early use of hand soldering (which is still used by some companies) through reflow soldering and tunnel ovens, to the more automated processes utilizing special heating processes such as induction and infra-red. Other processes also used to make the electrical joint(s) include ultrasonic bonding and resistance welding.

SECTION VI

INTERCONNECT PROCESSES AND SOLDERING MATERIALS

6.1 INTRODUCTION

The most common way to make the electrical joint is to solder it. Hand soldering, the simplest method, is also the slowest. This method requires the use of temperature controlled soldering irons, trained solder operators, and adequate procedures. The possibilities of human error are always present. Most companies have initiated more sophisticated processes, primarily to increase the number of solder joints that can be made for a given time, while reducing human error as much as possible.

6.2 REFLOW SOLDERING

Controlled resistance soldering (or reflow soldering as it is commonly called) is a microjoining process in which heat is produced by passing an electrical current through either the parts that are to be soldered, or a high resistance soldering tip. The amount of heat produced and the force applied at the soldering tip are controlled by the equipment being used. The solder required at the joint is applied in controlled amounts in the form of solder paste or solder preforms, or by reflowing the solder on tinned parts. Flux may or may not be used.

All that normally is required on the part of the assembly operator is positioning the parts to be soldered and actuating the solder head. The soldering tip is moved down to the work and a preset force is applied to the parts. At the right instant in the machine cycle, the power unit transmits electrical energy of a predetermined magnitude and time duration to either the soldering tips and parts or the soldering tip alone.

The advantages in controlled resistance soldering are close control of heat amplitude, heating time, force applied to parts, and amount of solder applied to the joint.

There are two basic types of controlled resistance soldering processes:

- 1) Single-point
- 2) Parallel gap

6.2.1 Single-Point Soldering

Single-point controlled resistance soldering is a versatile micro-joining process that can be used in a wide variety of "top side," or one-side, applications. The process is used extensively in joining various types of electronic components to printed circuit boards or thin films.

Single-point soldering tips resemble the electrodes used in split-tip resistance welding (Fig. 6-1). The single-point tip, however, is joined at one end to form a continuous, or "single-point," resistance element.

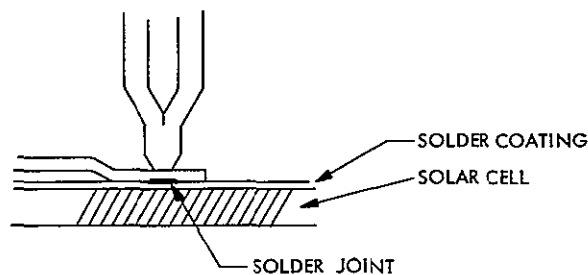


Fig. 6-1. Single-point soldering (Ref. 19)

The resistance to electrical current of the tip itself produces the heat needed to melt the solder and make the connection. During the electrical energy pulse to the tip, heat is transferred directly to the parts. Since all electrical current passes through the soldering tip, there is no danger of damaging the parts being joined by excessive current loads. The electrical resistance of the lead wires, ribbons, or other parts being joined has no effect on the amount of heat produced. However, heat-sink problems can be encountered depending upon the particular thermal characteristics of the parts involved. Consideration should be given to thermal properties during the design stage of assemblies.

In the process of making a single-point soldered connection, the soldering tip presses against the parts to be soldered and an electrical energy

pulse is passed through the tip for a time duration sufficient to bring the parts and solder alloy to the temperature needed for a reliable solder joint. After the proper temperature has been reached and the energy pulse to the tip has been interrupted, the tip remains in contact with the parts (dwells) long enough for the joint to cool and for the solder to completely solidify. The assembly is then repositioned by the operator for making the next soldered connection.

This process is especially well suited for making soldered joints with tinned interconnects. However, solder preforms of solder paste also can be used.

Either AC or DC power supplies can be used in single-point soldering.

6 2.1.1 Process Parameters (Approx)

Power Supplies

AC 60 or 1000 cps, 0.1 w to 200 w

DC 0.2 ws or 25 ws

Pulse Length

AC 50 ms to 1 sec

DC 1.5 to 700 ms

Tip Force

2 oz to 10 lb

Tip Size

0.005 to 0.025 in. sq

Total Thickness of Soldered Materials

0.015 in.

Maximum Material Thickness Ratio

5 to 1 preferred (not critical)

Typical Applications

Single-point soldering is used in a wide variety of "top side" applications involving relatively small diameters.

Advantages

- 1) The process is simple to use and easy to set up.
- 2) The process is "forgiving" of differences in materials and sizes.
- 3) When flux is used, it does not interfere with producing the heat needed for soldering.
- 4) Single-point tips can reach into very limited spaces.

Disadvantages

- 1) The process sometimes requires use of flux.
- 2) When flux is used, it has to be removed after soldering is completed.
- 3) The size and thermal properties of lands, pads, or runners that leads are being soldered to can affect the amount of heat required in soldering

When flux and solder preforms are to be used it is best to have the flux contained within the preform itself. Flux buildup on parts does not interfere with the soldering process. As a general rule, however, flux shortens soldering time.

When very small sections are being soldered, the force applied at the tip should be low so that the sections are not broken or damaged. The force used need only be sufficient to hold the parts in contact with the solder and base metal. Excessive tip forces can cause penetration through the interconnects. The tip force required usually is proportional to the thickness. Typically, a force of 2 oz is sufficient for a thickness of 0.001 in. diam whereas 2 to 3 lb might be required for a 0.010-in. thickness.

6.2.2 Parallel Gap Soldering

The parallel gap soldering process is almost identical in principle with parallel gap resistance welding. The heat required for making the solder joint is derived by passing an electrical current or pulse from one electrode through the materials being soldered and back to the other electrode. Heat is produced by the resistance of the parts themselves.

Also, in parallel gap soldering, two soldering tips approach the work-piece from one side and contact the interconnect at two points (Fig. 6-2).

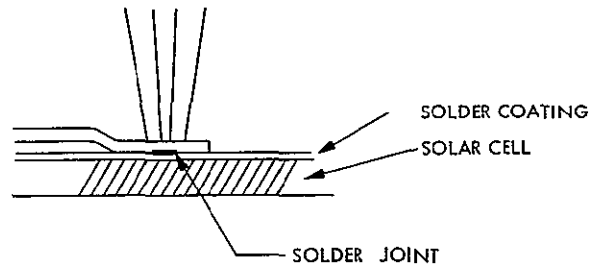


Fig. 6-2. Parallel gap soldering (Ref. 19)

Only one soldered joint, however, is made even though these are two tips. The size of the solder joint depends upon the gap width between tips. The force applied by each tip is the same.

With separately suspended or "loaded" tips the process is well suited for soldering uneven or bent interconnects. Normally, best soldering results are obtained when both leads and base materials are tinned or have a coating of solder. Solder preforms also can be used between the interconnect and the solar cell.

Since heat is produced by the resistance of the parts being soldered, the resistivity of the materials must be taken into account. Care must be exercised when flux is used as it interferes with electrical continuity and the resulting heat produced.

6.2.2.1 Process Parameters (Approx)

Power Supplies

AC 60 cps, 0.1 w to 200 w

DC. 0.2 to 50 ws

Pulse Length

AC. 0.1 to 2 sec

DC 5 to 700 msec

Tip Force

4 oz to 12 lb

Electrode Size

0.005 in. sq to 0.025 by 0.100 in.

Total Thickness of Soldered Materials

0.030 in.

Maximum Materials Thickness Ratio

3 or 4 to 1 preferred (not critical)

Advantages

- 1) The use of two soldering tips permits uneven or bent wires or ribbons to be soldered.
- 2) Large wires up to 0.030 in. diam can be successfully soldered.
- 3) Soldered joints can be inspected readily.
- 4) Wires as small as 0.003 in. diam can be soldered.

Disadvantages

- 1) The two-tip setup is not well suited for working in limited spaces.
- 2) The process isn't as fast as some other microjoining soldering processes.
- 3) Leads and runners should be pretinned.
- 4) Fluxing usually is necessary, especially for large parts.
- 5) Flux buildup can prevent current from passing through the parts.

If difficulty is encountered in getting sufficient heat to melt the solder, the possibility in 5), above, should be considered (Ref. 19).

6.3 TUNNEL OVENS

A tunnel oven is a conveyORIZED soldering system consisting of three process zones: A preheat zone, a hot (or soldering) zone, and a cooling zone. The temperature in both the preheat and the hot zones are independently controlled. The conveyor speed is adjustable.

6.3.1 General Construction

The general construction consists of removable tops on each processing zone for easy access to the heaters, blowers, thermocouple, and conveyor belt. The internal lines and baffles are made of 18-gauge stainless steel with heliarc welded seams. All external surfaces are constructed of heavy-gauge, cold-rolled steel. All exposed metal surfaces are painted with a high-temperature enamel. The process zones are insulated with 6 in. of high-temperature fiberglass material. Exhaust stacks with removable lids are provided for each zone. A port is also provided for the introduction of gaseous atmosphere. Entrance and exit baffles and flaps are provided to minimize hot losses. The baffles extend down to the top of the conveyor belt and cover the opening to minimize heat loss. The exterior of the oven is about 24 in. wide by 105 in. long and rests on a floor stand to provide a conveyor belt height of 32 in. above the floor. Instrumentation is affixed to the floor stand and is placed in such a manner that accessibility and influence of heat would not hamper or damage the instruments. All items are commercially readily available parts for fast replacement in case of damage, calibration of instruments, etc.

6.3.2 Temperature Control

An independent temperature controller and indicator for preheat and hot zone is utilized. Temperature control thermocouples are located in such a manner that optimum control of each zone can be maintained. The temperature controller operates off saturable core reactors with indicators and self-contained electronic thermocouple references (32°F). The thermocouple material is iron-constantan, 24 gauge. The saturable core reactors are mounted in a separate housing equipped with casters. West Instrument temperature controllers combined with Burton reactors are utilized in the temperature control circuit.

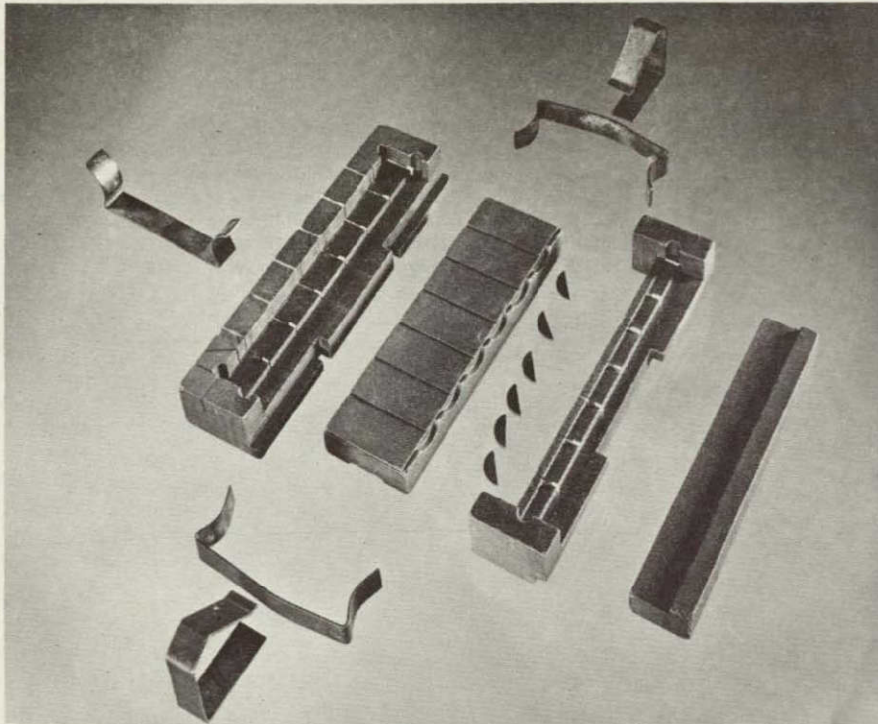


Fig. 6-4. Disassembled solder boat — early design

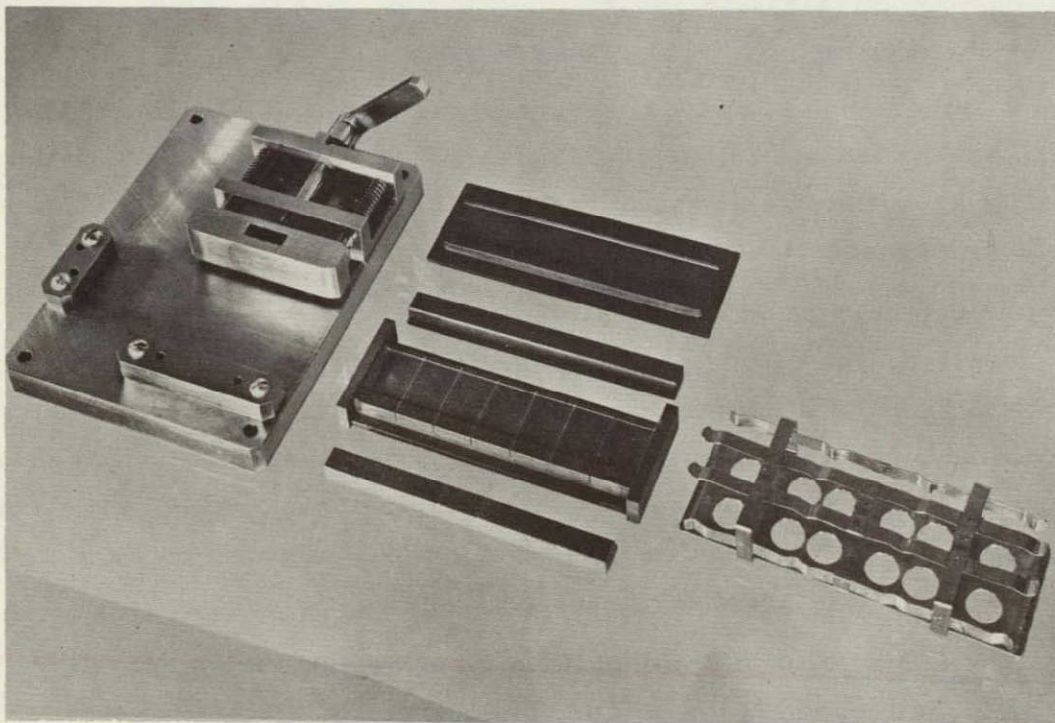


Fig. 6-5. Disassembled solder boat — new design

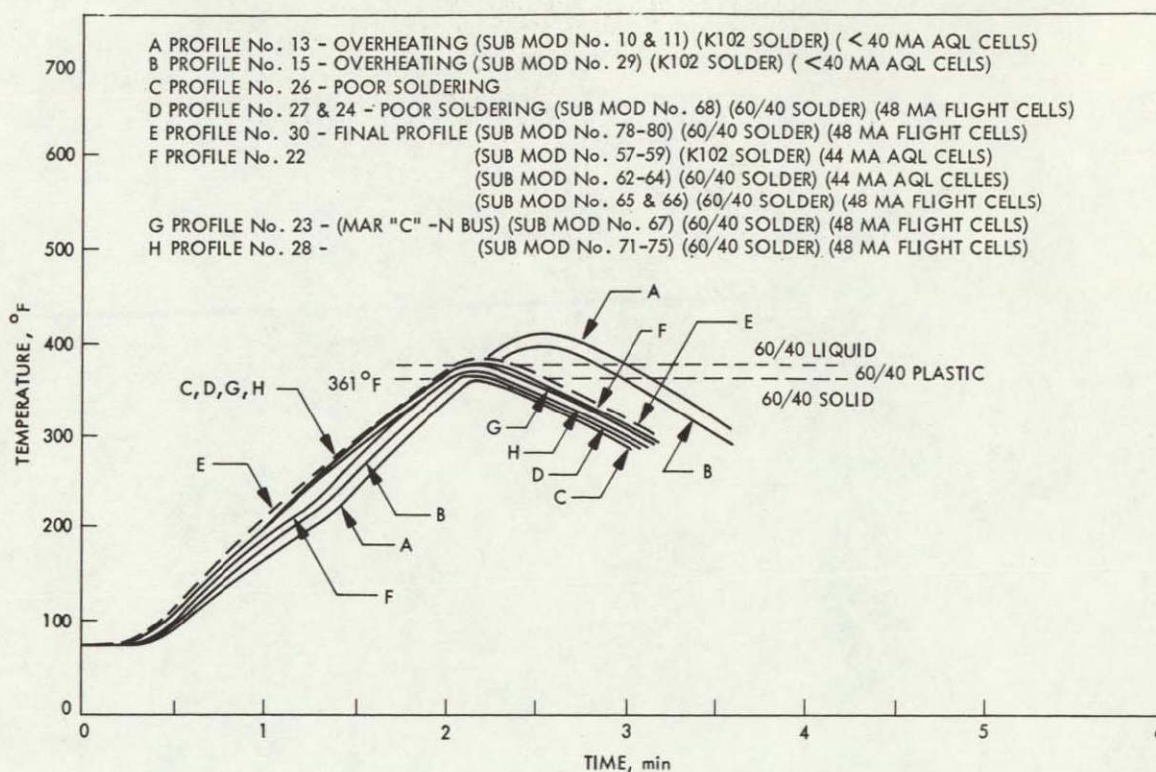


Fig. 6-3. Profile development

6.3.6 Soldering Boat

The Mariner 1964 solder boat assembly is shown disassembled in Fig. 6-4, and assembled in Fig. 6-5 using the spring clips to hold it together. A modification was initiated because of the many disadvantages in the Mariner 1964 boat. Some of these disadvantages are listed as follows:

- 1) As can be seen in Fig. 6-4, the solder boat is a complex assembly consisting of fifteen parts including five clips to hold it together and six small inserts that must be positioned in one of the four main blocks. The assembly time for the submodule-solder boat was 12 to 15 min because of this complexity and because a string had to be located and tied to provide the separation between the cells and the tabs on the negative bus bar (Ref. 20).
- 2) The solder boat did not hold the components firmly, thus there was a higher tendency for solder voids.

- 3) The mass of the solder boat was high, less mass would have permitted faster heating and cooling. Because of this large mass, the total oven travel time was 6 to 7 min. The time above the melting point of solder was 60 sec and the soldering temperature was approximately 410°F.
- 4) There was also a tendency for solder to buildup in areas on the backside of the submodule.
- 5) Use of teflon for cell spacers did not result in consistent cell spacing.

The modified Mariner 1964 solder boat was a distinct improvement over the original design. The improvements included a reduction in the travel time to 3 min, 10 sec with a reduction in the maximum temperature to 390°F, and a reduction in the assembly time to approximately 10 min. It still had the disadvantage of consisting of 15 parts. The components remained loosely held together with a tendency for solder voids and the solder continued to buildup in the areas in the backside of the submodule. In addition, the internal dimensions were oversize and worn, thus the new submodules could not be maintained within the print tolerances.

Also, a special conveyor carrier was required to properly position the boat on the tunnel oven conveyor belt.

Even with the improvements that resulted from the modification, it was felt that the shortcomings were excessive and a new design was started. The requirements were that it have a minimum of parts, be easily and rapidly assembled, have a low mass, and hold submodule components firmly and consistently without damaging them.

A significant improvement has been made in the manufacturing techniques and the quality of the submodules to be used on the Surveyor and Mariner 1967 programs. The redesign of the bus bars used on the submodule now permit the submodule to be used in more extreme environmental conditions such as occur on the lunar surface.

The assembly time has improved from the Mariner 1964 range of 12 to 15 min down to 5 to 6 min as a result of the new solder boat and the modified JPL tunnel oven. The combination of these two factors now yield a more

consistent and reliable submodule. In addition, it has accelerated the soldering process and hence, has reduced the time in which the solar cells are subjected to the soldering temperatures, thus there is less degradation of the solar cells during fabrication (Ref. 21).

Figure 6-6 compares the original Mariner 1964 soldering boat temperature profile with the modified Mariner 1964 boat and the Surveyor/Mariner 1967 soldering boat profile. These curves clearly illustrate the improvement in soldering time and the reduction of the time in which cells are at high temperature (Ref. 22).

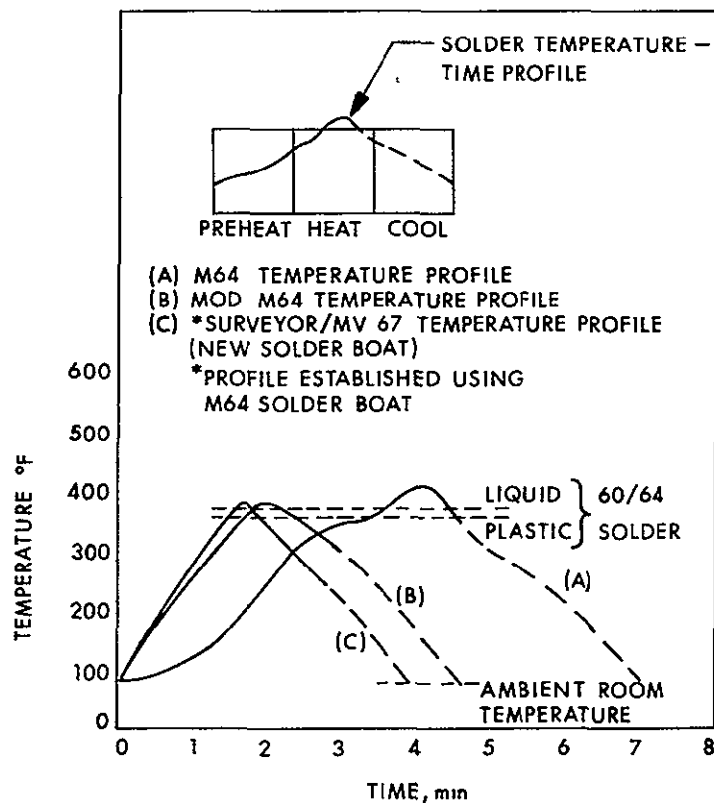


Fig. 6-6. Profile development — improved (Ref. 22)

6.4 RESISTANCE WELDING

The important major elements of the welding process are the following

- 1) Preparation of cells prior to welding
- 2) Welding operations for assembly of submodule arrays
- 3) Assembly of submodule arrays on panel

In 1), the P and N tabs are attached to the cells which are then assembled into submodules as shown in Fig. 6-7. In 2), the P tabs of one submodule are welded to the N tabs of another submodule, the process being repeated to form a desired array. In 3) the arrays of submodules are attached to the panel substrate, the arrays in turn being connected by welding.

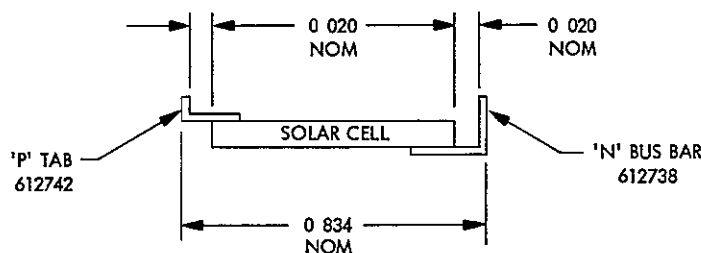


Fig. 6-7. Submodule subassembly before welding (Ref. 18)

Step 1) was facilitated by use of a fixture similar to that employed for fabrication of Ranger Block III solar panels. Compared to the Ranger fixture, the N bus bar spacer was altered to give a nominal cell-to-cell spacing of 0.020 in. Special bus bar locating slots were also incorporated.

A "Unitek" micro-spot welder was utilized. The copper electrodes were modified to increase the bearing area on the P tab and to provide better physical and visual access for the operator. The electrode tip pressure was set at 3 lb and the dwell cycle at 3 w-sec.

6.4.1 Conclusions on Resistance Welding

Based on the results achieved to date the following conclusions have been established.

- 1) The welding process is practical and lends itself to relatively simple, high-speed, low-cost, production methods

- 2) Reliable, sound welds can be attained with materials which are compatible with silicon solar cells
- 3) Negligible electrical degradation of cells is caused by welding
- 4) Multiple, on-panel welds are possible (Ref. 18).

6.5 ULTRASONIC BONDING

Ultrasonic bonding techniques have been utilized to form Al-to-Al interconnects in solar cells. To date, experiments have been only moderately successful. Some equipment problems have been solved and the special tips and wire necessary to continue have been received. The work is continuing with 3-mil Si-doped Al wire, with which bonds have been made. One group of bonds (material not identified) resulted in tensile strengths greater than the wire or the silicon (the bonds did not fail)(Ref. 6).

The most popular approach discussed appears to be the evaporation of an aluminum coating onto the silicon wafer, then ultrasonically bonding an aluminum interconnect to it. Other interconnect materials tried include gold wire and platinum wire. The companies involved in this area are not too eager to discuss their efforts in detail for various reasons ranging from proprietary to classified projects.

When fully developed, ultrasonic bonding will allow the use of aluminum as an interconnect on a solderless solar cell. The advantages are lighter weight with increased thermal capabilities. Some of the problems reported are cracks in the joints, aluminum disappearance at the joint, and the metallurgical degradation which occurs as a result of combining gold with aluminum under specific conditions.

6.5.1 General Description

Because no published reports were obtained with sufficient detail for solar cells, general information is hereby given.

Ultrasonic welding is accomplished by introducing vibratory energy into the materials in the area to be joined, in a plane essentially parallel to the plane of the interface. This is achieved by a transducer-coupling-tip system which converts high-frequency electrical power from a suitable source into

mechanical vibration and delivers it in the desired mode to the weld zone. In addition, a static clamping force is required to hold the materials in contact during the application of ultrasonic energy. The process is effective for producing spot type welds, overlapping-spot seam welds, and continuous-seam welds with a roller type welding tip.

Commercial equipment has been developed to operate in the frequency range of 15 to 100 kc per sec. Generally, the lower frequencies are used for equipment operating at high power, such as the 4000-w spot-type welding machine. In external appearance this welding machine resembles a resistance spot-welding machine, although the equipment is simpler to operate than an aircraft resistance spot-welding machine for aluminum. The only controls requiring adjustment are the power level, the clamping force and the weld pulse time. Somewhat higher frequencies are utilized in the spot type welding machine used for joining small components such as transistor leads, thin foils or instrument parts. A miniaturized 100-w welding machine developed for such purposes may be equipped with a microscope for precision joining of very fine wires and the like.

Continuous-seam welding equipment incorporates a rotating transducer coupling system, and the welding tip sometimes consists of a resonant disk attached to the end of an exponentially tapered coupler. Continuous vibratory power is applied longitudinally along the axis of the coupler, and the work either passes between two roller disks, one or both of which may be ultrasonically active, or it is carried under an active disk on a traversing table, as illustrated in Fig. 6-8. The seam welds produced by this method are continuous, and the joints are leak-tight to the limit detection by mass spectrometer leak testers.

Degreasing of the parts to be welded is usually essential, although other precleaning is generally unnecessary unless the material contains a heavy scale deposit. In such case, chemical cleaning or mechanical scale removal is necessary.

Basic research investigations of the ultrasonic welding mechanism are currently in process, and the significance of the various factors influencing the bonding is not yet fully understood. However, significant progress has been made in delineating the forces acting on the metal during welding and the metallurgical phenomena achieved. The applied vibratory energy combined with the

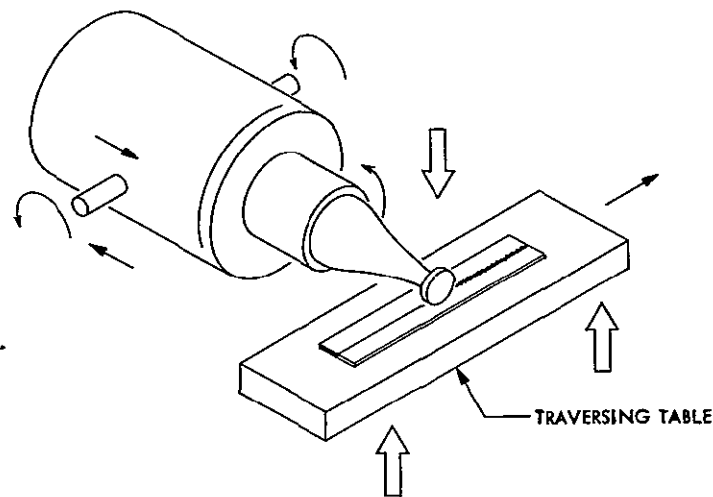


Fig. 6-8. Schematic diagram of traversing-table continuous-seam welding machine (Ref. 23)

normal static force induces rapid stress reversals along the bond interface, and mating surface films in the weld area are broken up and dispersed. Rupture of these films is accompanied by local plastic deformation, and substantial interpenetration of the weldment members may occur, although thickness deformation of the joint is usually negligible (generally less than 5%). The metallographic characteristics of a bond are determined by both the welding conditions employed and the relative properties of the materials and surface films

It has been established that a localized temperature rise occurs in the weld zone during ultrasonic welding, although interface-temperature measurements, coupled with metallographic observations, have shown no evidence of fusion. Furthermore, the magnitude of the temperature rise can be controlled within limits by appropriate selection of welding-machine settings.

Such localized heating of the contact surfaces lowers the stress level required for plastic flow and permits greater interpenetration and interfacial film disruption. It also introduces the possibility of diffusion reaction, such as oxide solution and solid-state alloying. However, conventional diffusion coefficients appear to limit the movement of thermally motivated atoms in the brief time available during formation of spot type weld, usually less than 1 or 1.5 sec. The available techniques for controlling the maximum temperature achieved can be used to minimize such diffusion reactions.

6.5.2 Ultrasonically Weldable Combinations

Ultrasonic welding permits the production of sound metallurgical bimetal junctions of structural integrity and/or good conductivity, with no cast structure, little or no interdiffusion and negligible formation of intermetallic compounds.

Table 6-1 shows graphically some of the combinations in which bimetal welds have been successfully achieved. The blank spaces do not necessarily mean that the combinations are impossible to join, in most cases, such welds have never been attempted. The metal elements listed in the table are understood to include the major alloys of these elements. For example, aluminum includes both structural and nonstructural aluminum alloys, copper includes several types of brass, such as gilding metal and cartridge brass, nickel includes the nickel-base alloys such as Inconel and Hastelloy, zirconium includes the more commonly used Zircalloys. Bimetal welds within each group are also possible, such as junctions between two types of steel of widely different properties (Ref. 23).

Table 6-1. Some dissimilar-metal combinations that have been ultrasonically welded (Ref. 23)

	Al	Cu	Ge	Au	Kovar	Mo	Ni	Pt	Si	steel	Zr
ALUMINUM		O	O	O	O	O	O	O	O	O	O
COPPER			O	O			O	O		O	O
GERMANIUM				O							
GOLD				O	O		O	O	O		
KOVAR					O		O	O			
MOLYBDENUM						O	O			O	O
NICKEL							O	O		O	
PLATINUM								O		O	
SILICON											
STEEL										O	O
ZIRCONIUM											O

6.6 INFRARED HEATING

Infrared heating techniques are being looked at more and more in the solar cell industry to replace the reflow soldering equipment. In addition, tunnel ovens are now available utilizing IR. As no reports were received in time for this report, a general description of IR heating will be given.

Infrared heating is the use of electromagnetic waves, in the infrared wavelength band, for radiant heat transfer. In simple terms, the old fashioned potbelly stove heated objects at a distance (not in physical contact) by the same means. In a heating sense, there are three elements to be considered in describing the heating system source or emitter, transport or control method, and finally, the absorber.

6.6.1 Energy Source

The energy source used for a typical application is a tungsten filament lamp of the quartz-iodine type. The operating temperature of the lamp is 3400°K maximum, and its spectral output ranges between 0.375 and 4.2 microns. The quartz-iodine lamp produces the maximum possible specific energy available in the non-exotic types of lamps. Arcs and plasmas produce more power for a given size, but they are also far more expensive and less flexible in their operation.

6.6.2 Reflector

The source is useless by itself because it radiates in all directions, and the intensity of radiation drops off as the square of the distance from the source. Some means is required to collect the radiation and direct it to where it can be used. For this purpose we employ mirrors or reflectors.

The reflector is shaped such that the energy leaving the source and striking its reflecting surface will be directed to a defined zone. This is shown schematically in Fig. 6-9. The workpiece is placed in the zone where it will absorb radiation and become hot.

The zone, often called the focal zone, may be either a spot or a long thin line. The shape and size of the zone is a function of the shape and size of the source and the reflector.

6.6.3 Object Heated

The last element in the heating system is the object being heated, which is a solder joint. In general, the emissivity of a soldering material is a function of wave length, temperature, alloy composition and surface condition.

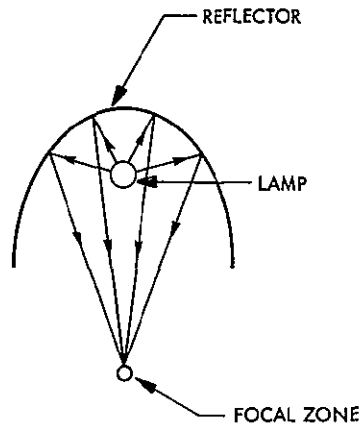


Fig. 6-9. Schematic of focused radiant heating system (Ref. 24)

A typical emissivity value for clean lead-tin solders is approximately 0.08, which is a relatively low value. However, the low emissivity is more than offset by the high radiant flux density that is available in concentrated infrared and by the relatively low temperatures required in soldering.

One of the most critical operating parameters in infrared soldering, and the one that contributes most to variations in emissivity (and therefore process repeatability), is the surface condition of the solder. As stated, the emissivity of clean solder is approximately 0.08. However, emissivity may vary from 0.18 due to a light oil film on the surface to as high as 0.6 for very heavily oxidized solder. Hence, strict control is necessary, not only with respect to the solder preform, but also tinned work pieces.

Surface uniformity is not difficult to control if a few precautions are taken. Good uniformity is obtained within a given lot when the solder preforms are stored in a tight container with a silica jell desiccant and not allowed to stand for more than 90 days before using. Variations from lot to lot may be compensated for by adjusting the heating power. In general, if the solder appears clean and bright, it is suitable for use in most cases. Also, the components to be joined should be as clean as the solder.

Other preparation techniques, such as fluxing and tinning, are the same as those used with any other heating method, and piece part design criteria are unchanged.

6.6.5 Disadvantages

By the same token, there are some disadvantages. Heating of massive parts is often slow and difficult. Infrared is a surface absorption phenomenon, and if the part is thick and has good thermal conductivity, the heating rate is slow.

The presence of flammable or heat-sensitivity materials near the joint can be troublesome. One way to get around this is to use suitable shielding to protect sensitive areas.

Reflective radiant systems require more scrupulous housekeeping than other heating methods. The reflector must be kept clean if it is to maintain long-term repeatability. Precautions must be taken to protect the heater from contamination during operation. Protection may take the form of suitable windows or purge systems to keep flux fumes away from critical parts. Maintenance schedules involving cleaning and inspection of cooling facilities must be well designed and adhered to (Ref. 24).

6.7 INDUCTION HEATING

Two companies have developed production type induction heating equipment for solar cells. These companies are Lockheed Electronics (Ref. 15) and Hughes Aircraft (Ref. 22).

Lockheed has developed a rotary table induction heating machine. The solar cell is assembled in its fixture with the interconnect and solder preform and then loaded into a position on the index table. The table is automatically indexed into the operating position, the power is automatically turned on, at the described power levels, and turned off after a specific time interval. As the table is indexed again, the cell moves to the unload position (Ref. 15).

Hughes has developed a conveyor type automatic induction soldering machine. Although not fully investigated, it is described as being capable of soldering 3 cells in parallel and 31 cells in series, one series after another (Ref. 22).

6.7.1 General Description

Induction heating is based on the principles of the alternating current transformer. When two electrical circuits are magnetically connected, an alternating current flowing in one circuit will cause a current to flow in the other, the magnitude of the current induced in the latter is a function of. (1) the magnitude of the primary current, (2) the ratio of the number of turns in the two circuits, and (3) the degree to which the two circuits are magnetically interlinked.

For simplicity, consider the fundamental electrical circuit used in induction heating. A source of alternating current is fed to the primary of a fundamental transformer, which is a heating coil, and this coil is magnetically coupled with the metal to be heated. When the alternating current is passed through the primary heating coil, a magnetic field is produced around this coil, its geometry depending upon the configuration of the coil proper. This magnetic field, changing in direction with the alternating current which produces it, induces voltage in any conductor placed in this field, if this conductor is part of a closed electric circuit it causes current to flow in that circuit.

This current acts the same as any other electric current and produces heat in the conductor proportional to the resistance of the electrical conductor at the frequency of the current flowing, and to the square of the current passing through the conductor. This heating effect is the same as that occurring in a simple resistance heater, the only difference is in the manner in which the current was introduced into the electric circuit. If the material making up the secondary of the transformer in which we are inducing heat energy is non-magnetic, and the magnetic coupling between the primary heating coil takes place in a non-magnetic medium such as air, which is the usual case, then the transformer analogy is complete. The resultant electric circuit can be looked upon as a transformer with relatively high leakage flux, since high degrees of magnetic interlinkage between two such circuits are difficult to obtain.

6.7.2 There are four characteristics associated with induction heating. These are (1) surface heating caused by the immediate secondary current flow on the surface of the work piece, (2) axial restriction within the confines of the coil, (3) rapid heat transfer to the work surface. This rapid heating is made

possible by the fact that the heat is developed directly within the metal, as with all electrical resistance heating, rather than being transmitted through the surface of the metal, as in torch- and furnace-type heating, (4) the energy is generated within the metal without any physical contact between the source of electrical energy and the metal being heated, that is, the medium of energy transmission, the magnetic field, can penetrate any non-metallic substance placed between the heating coil and the material being heated (Ref. 25).

6.8 OTHER SOLDERING APPROACHES

NASA Lewis Research Center has developed a solder bonding machine for use in CdS solar cells. It appears to be a conductive heating machine. Little information is available at this time.

6.9 COMPARISON OF SOLDERING METHODS

Table 6-2 is provided as a simple means to compare the various processes described.

6.10 SOLDERING MATERIALS

6.10.1 Solders

The soldering processes described in this report use solder of various compositions to produce the bond between the interconnect and the solar cell. The selection of any particular solder alloy composition must take into consideration not only the soldering temperatures but also the effects resulting from the solder alloy combining with the interconnect materials/coatings.

The most popular solder alloy compositions are SN 60 (60% SN and 40% Pb) and Eutectic SN 63 (63% SN and 37% Pb). These compositions are used when there is little or no concern for soldering effects.

Another popular solder composition is SN 62 (62% SN, 36% Pb and 2% Ag). This solder is used where thin silver coatings are used on the interconnect, or where the interconnect is pure silver, to greatly reduce the scavenging of the silver by the solder. The solubility of silver in a tin-lead solder is about 3% at 460°F (approximate soldering temperature); see Fig. 6-11 (Ref. 26). As a

Table 6-2. Comparison of soldering methods

	Advantages	Disadvantages	Automation possibilities
Hand soldering	<ol style="list-style-type: none"> 1. Low cost 2. Very flexible 3. Good for rework 	<ol style="list-style-type: none"> 1. Requires skilled operators 2. Length of time heat is applied (even with temperature controlled iron) is critical and is operator dependent 3. Tool handling techniques are critical 4. High potential rejection rate 5. Not a repeatable process 	Poor. Can make only one joint at a time.
Reflow soldering (parallel gap, single heated probe, etc.)	<ol style="list-style-type: none"> 1. Controls heat energy input 2. Controls time of heat application 3. Controls contact pressure 4. Flexible 5. Repeatability 6. Uniformity 7. Semi-skilled operators 8. High production rate 	<ol style="list-style-type: none"> 1. High equipment costs (\$500-\$2000) 2. Requires careful pre-evaluation 3. Requires careful preparation of welding equipment 4. Requires special fixtures and welding tips 5. Requires careful positioning of Electrodes on workpiece 	Fair. Requires a separate power supply for each set of electrodes. Can make only one joint with each set of electrodes.
Tunnel oven	<ol style="list-style-type: none"> 1. Heat input is controlled 2. Heat exposure time is controlled 3. Can use unskilled labor 4. Can solder several cells together at one time 5. Repeatable 6. High production rate 	<ol style="list-style-type: none"> 1. High equipment costs (Thousands of \$) 2. Requires pre-evaluation for temperature and time parameters 3. Requires assembly of cells in Boat including fluxing, solder preforms and interconnects 4. Requires long warmup time 5. Requires long time exposure to heat (minutes not seconds) 6. Solder flow must be restricted to pre-designated areas to ensure good joint 7. Requires design of Boats to ensure no movement of cells to tabs 8. Requires additional amounts of solder and flux 	Good. A complete array (row) can be soldered simultaneously. Requires other techniques to solder between arrays. Could be improved by using infrared heating source.

Table 6-2. Comparison of soldering methods (continued)

	Advantages	Disadvantages	Automation possibilities
Induction heating	<ol style="list-style-type: none"> 1. Heat input is controlled 2. Heat exposure time is controlled 3. Can use unskilled labor 4. Can solder several cells at a time 5. Solder time is in seconds 6. No contact with workpiece is necessary 7. Joint takes the shape of the coil 8. Repeatable 9. High production rate 	<ol style="list-style-type: none"> 1. High equipment costs (Thousands of \$) 2. Requires pre-evaluation for temperature and time parameters 3. Requires pre-assembly of cells in fixtures 4. Requires design of coils and fixtures to be compatible with interconnect 5. Heating of solder joint continues after coil is de-energized due to the higher temperature of the surrounding metal mass 6. Requires control and restriction of solder flow to designated areas 	Very good. A complete module (rows of arrays) could be soldered simultaneously and sequentially.
Infrared techniques	<ol style="list-style-type: none"> 1. Radiant energy input is controlled 2. Time of energy input is controlled 3. Very short time parameters 4. Immediate "on" and "off" capabilities 5. Can be adapted to tunnel ovens 	<ol style="list-style-type: none"> 1. High equipment costs (\$500-\$2000) 2. Requires pre-evaluation for temperature and time parameter tolerance 3. Requires design of fixtures and filters to be compatible to interconnect 4. Requires shielding for safety and to protect sensitive parts 5. Requires design of fixtures to prevent movement of interconnects of cells 	Appears very good. A complete module (rows of arrays) could be soldered simultaneously and sequentially.
Ultrasonic bonding	<ol style="list-style-type: none"> 1. No solder or flux required under specific conditions 2. No heat required 3. Joint takes the shape of the sonotrode (TIP) 	<ol style="list-style-type: none"> 1. High initial equipment costs (Thousands of \$) 2. Requires pre-evaluation for pressure and frequency 3. Requires preparation of cells in fixtures 	Appears very good. A complete module (rows of arrays) could be welded in sequentially).

Table 6-2. Comparison of soldering methods (continued)

	Advantages	Disadvantages	Automation possibilities
Ultrasonic bonding	4. Currently in use in the electronic industry for bonding aluminum leads to silicon wafers	4. Requires design of sonotrode and fixtures to be compatible to interconnect 5 Requires metalized coating on silicon if bonding aluminum to silicon	

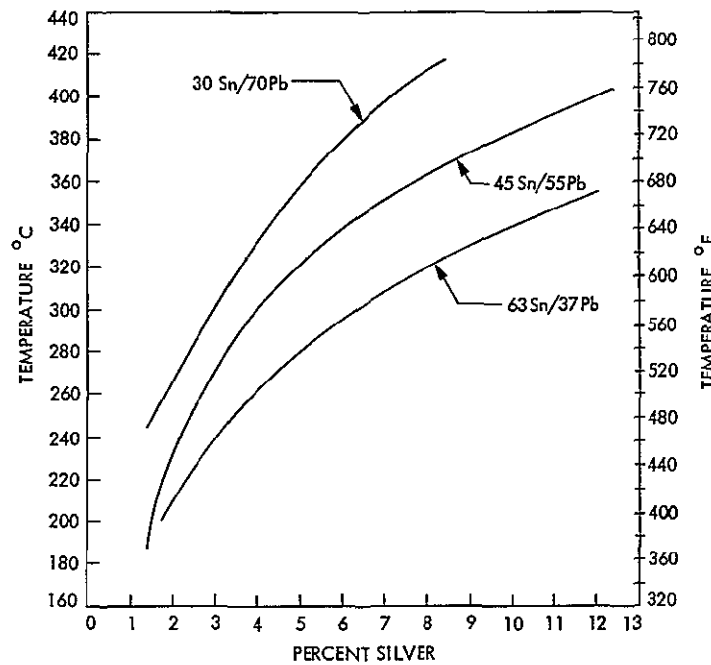


Fig. 6-11. Solubility of silver in tin-lead solders at various temperatures (Ref. 26)

result, the silver-bearing solder reduces the scavenging effects without adversely affecting the solderability. The use of higher percentages of silver in the solder would increase the soldering temperatures.

An indium-bearing solder such as Alpha No. 235, is used where thin gold films are employed to reduce the scavenging of the gold by the solder. The melting point of this solder is advertised as 304°F (151°C) which makes it useful for soldering to temperature sensitive materials. Actual tests conducted with this solder alloy (see Table 6-3) reveal that the strength of the resulting solder joints are less than half of the strength of solder joints made with 60/40 solder (Ref. 27). The use of low temperature solders such as indium-bearing solders may require changing to a low temperature flux. This change will depend upon what the actual melting and soldering temperatures are. One verbal contact reported the use of an indium-bismuth solder alloy. Alpha metals has a solder alloy (No. 8) which is a composition of indium, bismuth, and tin in addition to some other elements. It is reported as having a melting point at 100°C – 110°C.

Table 6-3. Comparison of Alpha 235 and 60/40 solder (Ref. 27)

		Strengths of joints (lb) formed with Alpha 235 solder, Alpha 709 flux at				
Bath	Substrate	163°C (325°F)	177°C (350°F)	190°C (375°F)	204°C (400°F)	Average
A	N ₁	19.0	13.0	11.3	13.5	14.2
	Ag	19.8	14.7	13.5	13.0	15.3
B	N ₁	19.7			15.8	17.8
	Ag	15.3			15.3	15.3
D	N ₁	12.0	16.5	13.8	9.5	12.9
	Ag	15.8			9.8	12.8
E	N ₁	15.5	11.5	15.3	11.5	13.5
	Ag	17.0	16.3	12.0	8.0	13.3
F	N ₁					
	Ag					
		Strengths of joints (lb) formed with 60% Sn-40% Pb solder, Alpha 709 flux at				
		232°C (450°F)	245°C (475°F)	260°C (500°F)	274°C (525°F)	Average
A	N ₁	41.5	34.5	26.0	23.5	31.4
	Ag	35.5	36.3	42.5	35.0	37.4
B	N ₁	31.8	30.3	26.5	25.5	28.5
	Ag	30.8	28.8	30.8	36.8	31.8
D	N ₁	34.8	27.0	34.3	20.0	29.0
	Ag	36.0	35.3	38.8	27.0	34.3
E	N ₁	28.3	31.3	30.8	33.3	31.0
	Ag	34.0	42.3	29.8	29.0	33.8
F	N ₁	37.5	39.5	36.3	41.5	38.7
	Ag	29.0	40.8	42.5	34.3	36.6
Bath Compositions						
Bath	g/l KAu(CN) ₂	g/l Other additives				
A	15	Organic Acid + Na Salt 100				
B	8	Cobalt <1.0, organic acid + K salt 50				
C	8	Cobalt 1.0, organic acid + K salt: 50				
D	8	Nickel. <1.0, organic acid + K salt. 80				
E	8	Nickel. 1.0, organic acid + K salt. 80				
F	8	Nickel: >1.0, organic acid + K salt. 80				

6.10.2 Fluxes and Cleaning Solvents

Fluxes are used to chemically clean the tarnish from the surfaces to be joined by soldering prior to the solder melting during the soldering (or tinning) operation. The fluxes hold the contaminants in suspension and float to the surface of the molten solder. Proper selection of fluxes will not only leave the surface clean for the molten solder, but also will improve the wetting characteristics of the surfaces and the related solder spread. The flux residues are then removed after the solder has solidified. The flux residue removal is critical where active fluxes are used. Therefore, the selection of cleaning solvents becomes dependent upon the fluxes used. The most popular fluxes appear to be activated rosin fluxes such as Kester 1544, with both organic and inorganic fluxes also being used. The cleaning solvents include alcohols (isopropyl and ethyl), deionized water, trichlorethane, MEK, acetic solutions, dilute HCL, and water base detergents. There doesn't appear to be any set pattern in the solar cell industry with respect to the use of fluxes or cleaning solvents. One verbal contact reported the use of Alpha 709 as a solder; it is actually a water soluble organic flux. Another verbal contact reported the use of a detergent as a flux. It is occasionally used as a cleaning solvent. The impression is that this industry takes these items for granted.

SECTION VII

TESTS

SECTION VII

TESTS

7.1 APPLICABLE TESTS

Tests are performed to ascertain that the fabricated module is capable of meeting the design requirements. The parameters of the tests involved are established at limits which insure meeting the design objectives.

The tests and associated parameters may be as follows:

- 1) Acoustic Noise up to 150 db (Ref. 27)
- 2) Sinusoidal Vibration. Vibration applied along each of three mutually perpendicular areas (Ref. 15)

5 to 14 Hz	0.5 in D.A.
14 to 400 Hz	5.0 g
400 to 2000 Hz	7.0 g

Sweep rate of 3 min per octave
- 3) Random Vibration. Vibration applied for five (5) minutes along each of the three axes at the levels shown below (Ref. 15)

20 to 400 Hz	0.017 g^2/Hz
400 to 2000 Hz	0.0196 g^2/Hz
Composite Level	13.0 g
- 4) Boost shock of 150 ± 15 g at half sine or 190 ± 20 g saw tooth, 0.5 to 1 msec in both directions
- 5) Cold thermal vacuum tests to a temperature of $-310^\circ F \pm$ at a vacuum of 10^{-5} mmHg for 20 hr
- 6) Hot thermal vacuum tests to $+270^\circ F \pm 10^\circ F$ at a vacuum of 10^{-5} mmHg for 100 hr
- 7) The thermal shock may be performed by immersing the submodules into liquid nitrogen (LN_2) for 10 sec after which they are immediately removed and dipped into boiling distilled water for 10 sec. This constitutes one cycle of the test. Each submodule is subjected to either three or five cycles (Ref. 27)

- 8) Electrical performance tests consist of illuminating the cell with a tungsten light source with an equivalent solar intensity of 100 mw/cm^2 and a color temperature of 2800°K . The uniformity of light intensity is within $\pm 1\%$ over the area of the cell or submodule. The solar cell submodule electrical performance test fixture temperature is maintained at $28^\circ\text{C} \pm 2^\circ\text{C}$ by using a controlled temperature water bath. For evaluation purposes, the cell or submodule current output is measured at a voltage of 0.485 v. This voltage and corresponding current measurement are coordinates at, or close to, the cell/submodule maximum power point, and therefore provide a reference for evaluating a cell or submodule power capability (Ref. 20). Typical requirements would be established for the current flow which is convertible to percent efficiency.

REFERENCES

REFERENCES

1. "Solar Cell Cover-Glass Development;" Third Quarterly Report; Ion Physics Corporation, Burlington, Massachusetts.
2. Mandelkorn, J.; "Improved N on P Silicon Solar Cells;" NASA Technical Memorandum, NASA TM X-52102; NASA Lewis Research Center; Cleveland, Ohio
3. Reynard, D. L., and Andrew, A.; "Improvement of Silicon Solar Cell Performance Through the Use of Thin Film Coatings;" Applied Optics, January 1966 (by permission of Optical Society of America)
4. Solar-Cell Integral Cover-Glass Development; Report No. 03-67-51, Texas Instruments Inc., Semiconductor-Components Division, P. O. Box 5012, Dallas, Texas.
5. Integral Glass Coatings for Solar Cells, Final Report; Contract No. NAS 5-3857; Hoffman Electronics Corp., Semiconductor Division, El Monte, California.
6. "Improved Solar Cell Contacting Techniques;" First Quarterly Report; Ion Physics Corp., Burlington, Massachusetts.
7. Research and Development Study on Improvement of Advanced Radiation-Resistant Modularization Techniques, Final Report; Contract NAS 5-3812; Radio Corp. of America, Direct Energy Conversion Dept.; Mountaintop, Pennsylvania.
8. Fabrication Feasibility Study of a 20-Watt per Pound Solar Cell Array, D2-23942-5; The Boeing Co.; Seattle, Washington.
9. Brozdowicz, Z.; "Thermal Tests of Two Types of Adhesives for Bonding of Solar Cell Filter to the Cell;" Technical Memorandum No. 342-25, JPL; Pasadena, California.
10. Anderson, J. E.; Adhesives for the Installation of Solar Cells on Photovoltaic Concentrating Panels; Aerospace Division, The Boeing Co.; Seattle, Washington.
11. MV'67 Solar Panel Material Test; Report No. 7049-MTR; Electro-Optical Systems, Inc.; Pasadena, California.
12. Advanced Technology of Interconnections in Microelectronics; NASA Work Unit; 125-25-03-01-25, ERC-NASA.
13. Metallurgical Study of Laminated Metallization Systems for Silicon Integrated Circuits; NASA Work Unit; 125-25-01-43-25, ERC-NASA.
14. Thin Continuous Gold Films for Metal Base Transistors; NASA Work Unit; 125-25-02-43-25, ERC-NASA.

REFERENCES (contd)

15. Solar Presentation; LEC to JPL; May 2, 1968; and Lockheed Electronics Co. Advanced Design, Solar Cell Panel (courtesy of K. A. Ray, Lockheed Electronics Co.; Sunnyvale, California).
16. MV'67/Surveyor Submodule Fabrication; Report No. 7049-FR; EOS, Pasadena, California.
17. Various Documents on Solar Cell Interconnects (courtesy of J. D. Gum); Spectrolab; Sylmar, California.
18. Fabrication of a Solar Cell Panel With Welded Submodules; Report No. WA 4350; EOS, Pasadena, California.
19. Larson, R. B.; Microjoining Processes for Electronic Packaging; Assembly Engineering; October 1966 (by permission of Hitchcock Publishing Co., Wheaton, Illinois).
20. Surveyor/Mariner '67 Silicon Solar Cell Submodule; Report No. 7050-DQR-1; EOS, Pasadena, California.
21. Flexible Integrated Solar Cell Array; Report No. SSD 70628R; Hughes Aircraft Co., Space Systems Div.; El Segundo, California.
22. Yasui, R. K.; Solar Cell Submodule Design and Assembly; Jet Propulsion Laboratory; Pasadena, California.
23. Patthoff, W. C.; Thomas, J. G., and Meyer, F. R.; "Ultrasonic Welding of Dissimilar Metal Combinations;" Welding Journal; February 1960 (by permission of American Welding Society; N Y., N Y).
24. Various Documents in Infrared Heating (courtesy of B. J. Costello); Argus Engineering Co.; Hopewell, New Jersey.¹
25. Cable, W. J.; Induction and Dielectric Heating; Copyright 1954, Reinhold Publishing Corp.; New York, New York (by permission of Van Nostrand-Reinhold Co.).
26. "Plating," Journal of American Electroplating Society; November 1965 (by permission of American Electroplaters Society).
27. "Silver Bearing Soft Solder;" Technical Bulletin 6a-36; (by permission of Alpha Metals, Inc.; Jersey City, New Jersey)
28. Yasui, R. K.; "Composite Solar Cell Matrix is Reliable, Lightweight, and Flexible;" NASA Technical Brief 67-10503.

¹ This reference also includes excerpts from:

"Soldering with Infrared Heating;" The Western Electric Engineer; July 1964 (by permission Western Electric Co.).

APPENDIX A
VERBAL CONTACTS

APPENDIX A
VERBAL CONTACTS

	<u>Company Name and Address</u>	<u>Contacts</u>	<u>Telephone No.</u>
1.	Battelle Memorial 505 King Columbus, Ohio	Clay Garton	(614) 299-3151
2.	Bell-Howell Res. Lab. 306 N. Sierra Madre Villa Pasadena, California	Dr. Bernard Ross	(213) 795-8601
3.	Central Lab 4501 N. Arvin Drive El Monte, California	Kay Ling	(213) 579-0700
4.	De Wire Fabricating Lowell, Missouri	Ken Scagl	(617) 458-8709
5.	EG & G Bedford, Massachusetts	J.E. O'Brien	(617) 271-5235
6.	Electrovert Inc. Mt. Vernon, New York	Don Daniels	(914) 664-6090
7.	Engineered Mach. Bldg. 2632 Frontage Road Mountain View, California 94040	M. Penninges	(415) 968-1788
8.	S. J. Industries 6009 Farrington Avenue Alexandria, Virginia 22304	Richard F. Julius	(703) 751-5400
9.	Fairchild Hiller Germantown, Maryland	Tom Berry	(301) 948-9600
10.	Fairchild Hiller Mountain View, California	Don Munoz	(415) 962-2804
11.	Hewlett-Packard Mountain View, California		(415) 969-0880

	<u>Company Name and Address</u>	<u>Contacts</u>	<u>Telephone No.</u>
12.	G.E. Spacecraft Dept. VFSTC, Room 2614 P.O. Box 8555 Philadelphia, Pennsylvania	Floyd A. Blake	(215) 962-4129
13.	G.E. Woods 2415 So. Manchester Anaheim, California	Al Little	(714) 633-9370
14.	General Telephone Electromc Laboratory Bayside, New York	Gary Argue	(212) 225-5000
15.	Heliotex 12500 Gladstone Sylmar, California	Gene Ralph	(213) 365-6301
16.	Hughes A & E Newport Beach, California	Art Edmonds	(714) 548-0671
17.	Hughes Aircraft Box 90919 Los Angeles, California 90009	W. D. Brown	(213) 648-4774
18.	International Rectifier 233 Kansas El Segundo, California	Don Pen	(213) 678-6281
19.	Ion Physics Corp. Burlington, Massachusetts	Alan Kirkpatrick	(617) 272-2800
20.	Lockheed Aircraft Co. Pinewood Drive San Jose, California 95129	Larry Chedester	(408) 742-8749
21.	Martin Company P.O. Box 179 Denver, Colorado 80201	John H. Martin	(303) 794-5211 Ext. 4417
22.	McDonnell-Douglas 5301 Bolsa Avenue Huntington Beach, California 92646	Mr. Ron D. Stevens	(714) 897-0311

	<u>Company Name and Address</u>	<u>Contacts</u>	<u>Telephone No.</u>
23.	MIT Lincoln Lab	Dr. F. William Sarles, Jr.	(617) 876-6900
24.	NASA Goddard SFC Space Power Tech. Branch Code 716.1 Greenbelt, Maryland 20771	John W. Fairbanks	(301) 982-6841
25.	NASA -Huntsville Huntsville, Alabama	L.W. Brantly Jim Miller	(205) 876-9551 (205) 876-6848
26.	National Cash Register Dayton, Ohio	Tom Sherby	(513) 449-2000
27.	Philco-Ford Corp. M/S 973 3825 Fabrian Way Palo Alto, California 94304	D.C. Briggs	(415) 326-4350 Ext. 6183
38.	Quantum Devices Inc. 1820 Mills Avenue El Paso, Texas 79901	John S. Skarman	(915) 532-4651
29.	RCA Princeton, New Jersey	M. Wolf	(609) 448-3400 Ext. 2570
30.	Ryan Aeronautical Co. San Diego, California	W.M. Cattrell	(714) 296-6681 Ext. 8485
31.	Smithsonian Inst. Science Info. Exchange 209 Madison National Bank Bldg. 1730 M. St. N. W. Washington, D. C. 20036	Mr. Liedman	(202) 381-5711
32.	Sonobond Corp. W. Chester, Pennsylvania	Dave Kirkwood	(215) 696-4710
33.	Sperry Rand Huntsville, Alabama	Jerry Bruno	(205) 539-3771
34.	Sylvania Mountain View, California	M.N. Halus	(415) 966-2654
35.	Texas Instruments Dallas, Texas	Ray A. Vineyard	(214) 238-2011 Ext. 3191

	<u>Company Name and Address</u>	<u>Contacts</u>	<u>Telephone No.</u>
36.	TRW Space Technology Lab 1 Space Park Redondo Beach, California 90278	Albert C. Lee	(713) 591-3133 Ext. 3243 (Houston)
37.	TRW Redondo Beach	Murry Brown	(213) 679-8711
38.	Unitek 950 Royal Oaks Drive Monrovia, California 91016	Pete Bullock	(213) 359-8361
39.	Westinghouse Pittsburg, Pennsylvania	L.J. Owsley	(412) 255-3322

APPENDIX B
LIST OF DOCUMENTS COLLECTED

APPENDIX B
LIST OF DOCUMENTS COLLECTED

- 1) NASA SP-32, Vol 3, June 1963
Telstar I
- 2) Surveyor SC 5 - SC 7, Solar Panel Electrical Design Analysis, June 1966
R.E. Ross EOS
- 3) Solar Power Systems - Manufacturing Process Standards - Various
Lockheed Elec. Co.
- 4) N64-13903 Research and Development Techniques for
Fabrication of Solar Concentrators
EOS Report 1587 Final 27 December 1961
- 5) N64-27886 Installation of Solar Cells on Photo Voltaic
Concentrator Panels
Boeing for JPL 950270 Document D2-35167
- 6) N66-11228 Investigation of Resinous Materials for Use as
Solar Cell Cover Glass Adhesive
Joseph G. Haynos
Goddard Space Flight Center
X-716-65-369
- 7) N64-28643 Evaluation of Optical Properties and Environmental
Stability of Solar Cell Adhesives
R. E. Mouri, April 1964
Lockheed Missiles and Space Center
LMSC AO 34229
- 8) AD 440016 VT/4060
EG&G Report No. B-2763
AF 33(657) - 12291
- 9) AD 406818 Dendritic Silicon Solar Cell Panel
Westinghouse Electric Corporation
Task No. 817301-29
AF 33(657)-9820

- 10) AD 270131 Solar Cell Array Optimization
RCA November 1961
Techmcal Report 61-11
- 11) AD 274841 Solar Cell Array Optimization
RCA February 1962
Techmcal Report 61-11
- 12) AD 439605 Solar Reflector Foaming Tech.
GER 11494 February 1964
AF 33(657)-10165
Goodyear Aerospace
- 13) JPL 6B-8107-63 Rigidization Analysis of Wire Film Materials
GER 11117
E. Rott Mayer
Goodyear Aerospace
- 14) DIN 68SD4233 Thin Film Solar Cell Module Development,
Cadmium Sulfide Cell
F. A. Blake and M. R. Stahler
G. E. NAS 3-10605
- 15) JPL 6B-8111-64 The Electrical Characteristis of Irradiated
Silicon Solar Cells as a Function of Temperature
B. T. Cunningham, Robert L. Sharp, and
Luther W. Slifer
Goddard Space Flight Center
- 16) JPL 342-15 Observations on Snap 2 and Snap 10A Nuclear Power
Systems
E. L. Leventhal
- 17) JPL 342-32 Design Analysis and Reliability Study of Ranger
Block III Electronic Conversion Equipment
E. N. Costogue
- 18) JPL 342-40 Calibration of Secondary Standard Solar Cells
Against the Balloon Flight Calibration Primary
Standards
SM 5-7 and SM 3-15
D. W. Ritchie

- 19) JPL 342-41 Ranger Block III - Mark IV
Solar Panel - Final Type
Approval Testing
- 20) Submodule High Temperature Test Report
A.O. Bridgeforth
EOS 7050-TR-2
- 21) Surveyor Solar Panel Sandwich Flexure Tests
With Active Solar Cells
T. R. Wheeler
EOS 7050-TR-11 11 May 1967
- 22) Surveyor Solar Panel Sample Panel Test Report
JPL Contract 951488
EOS No Number
R. L. Moor
- 23) ARL 67-0190 Research on The Mechanism of the Photovoltaic
Effect in High Efficiency CdS Thin Film Solar Cells
Clevite Corporation September 1967
AF 33(615)-5224
- 24) ARL 67-0282 Fabrication of Cadmium Sulfide Thin Film Solar
Cells for Space Vehicle Testing
Clevite Corporation December 1967
AF 33(615)-3253
- 25) NASA CR 72382 CdS Solar Cell Development
Clevite Corporation February 1968
NASA-Lewis NAS 3-9434
- 26) NASA CR 72159 Study of Thin Film Large Area Photovoltaic
Solar Energy Converter
Clevite Corporation December 1966
NASA-Lewis NAS 3-8502
- 27) Paper The History, Design, Fabrication and Perfor-
mance of CdS Thin Film Solar Cells
F. A. Shirland
Clevite Corporation 19 May 1966

- 28) The CdS Thin Film Solar Cell
F. A. Shirland
Clevite Corporation 8 March 1968
- 29) AD 815425 Improved CdTe Solar Cell and Array Environmental Effects Investigation
GE Semi-conductor Division May 1967
AF 33(615)-67-C-1485
- 30) AD 653184 Direct Energy Conversion in USSR Soviet Solar Concentrators.
30 November 1966
- 31) AD 652-799 An Investigation of Industrial Practices in Joining Foils with Experimental Investigation in Pressure Welding Foil Aluminum
University of Texas
January 1961
- 32) Large Area Solar Array Design
JPL Contract 951653
Boeing Company October 1967
Parts I, II, and III
 - (1) Reorder No. 67-704
 - (2) Reorder No. 67-705
 - (3) Reorder No. 67-706
 - (4) Process Document D2-113354-1
- 33) GE Package - Documents and Drawings
Courtesy of K.L. Hansen
GE - Advanced Space Power Division
Valley Forge Space Technology Center
- 34) N67-38493 Lightweight Solar Panel Interconnects
EOS 7088 August 1967
- 35) N66-27741 Materials and Methods for Large Area Solar Cells
RCA January 1966
NASA-Lewis NAS 3-6466

- 36) N67-22856 Aluminum-to-Copper Koldweld Joints for Snap-8
Electrical Terminal Applications
Aerojet-General July 1965
- 37) Ion Implantation as a Production Technique
J. T. Burrill, W. J. King, S. Harrison and
P. McNally
IEEE January 1967
- 38) Experience in Fabricating Semi-conductor Devices
Using Ion Implantation Techniques
W. King, J. Burrell, S. Harrison, F. Morten
and C. Killett

1965
- 39) General Specification Guide for Solar Cell Covers
Optical Coating Lab. Inc. January 1966
- 40) General Specification Guide for OCLI SI-100
Mirrors for Use as Thermal Control Devices
Optical Coating Lab. Inc. October 1966
- 41) Creativity With Thin Film Optical Coatings
Optical Coating Lab. Inc.
- 42) Brochure
Ion Physics Corporation
- 43) Proprietary Package from Martin
Marietta Corporation
Repairable Solar Cell Interconnect
- 44) Application of Silver-Cerium Contacts
H.W. Brandhorst
NASA-Lewis
- 45) Brochure
International Rectifier

- 46) N67-26520 Investigation of Contact Failures on Resistors
R. Gong
Philco Microelectronics Division
NASA Contract No. NAS 5-9322
October 1966
- 47) 3B-5126-65 High Voltage Solar Cell Array Segment
Westinghouse April 1965
AF 33(615)-3462
- 48) 3B-5130-66 Thin Film Photovoltaic Cell Array Investigation
GE May 1966
AF 33(615)-2695
- 49) 3B-5138-67 Production of Lightweight Photovoltaic Silicon
Solar Cells
Heliotek Report 9
NAS 7-484 1 February 1967
- 50) Performance of Very Thin Silicon Solar Cells
E. L. Ralph March 1967
- 51) 3B-5144-67 Review and Evaluation of Past Solar Cell
Development Efforts
RCA June 1967
NASW-1427
- 52) 1B-0458-65 Final Report Jet Propulsion Laboratory Purchase
Order
BK4-312938
Heliotek Report 1 1 February 1965
- 53) 3B-5107-64 Radiation Damage in Silicon
RCA October 1964
NAS 5-3788
- 54) 3B-5100-64 Materials and Methods for Large Area Solar Cells
RCA April 1964
NAS 3-2796

- 55) 3B-5163-68 Photovoltaic Power Systems on Flight Spacecraft
Nimbus 2
NASA CR -62045
Document 68SD4222 23 February 1968
GE
- 56) 3B-5115-66 Experimental Study of Coatings for Temperature
Control of Solar Cells
Philco WDL Division June 1966
NAS 7-409
- 57) 3B-5128-64 Positive Deployable Solar Arrays
Fairchild Status SSD 65.0
- 58) The Use of Vacuum Deposited Coatings to Improve
The Conversion Efficiency of Silicon Solar Cells
In Space
Alfred Thelen 1962
- 59) Proprietary Package from Applied Technology
Incorporated
W. C. Dunkerly
(1) Improved Solar Cell Cover Glass Bond
(2) Independent Research and Development
Report Solar Battery Pack Operational Test
TR No. 650-67-128 October 1967
(3) Kovar Substrate Soldering--Temperature
Measurements During Induction Heating
650-67-138
(4) IR&D Quarterly Review
1810-68-014
(5) Screm Cloth Experiment II
650-67-123
- 60) Bibliography--Solar Arrays and Associated
Technologies
Fairchild-Hiller April 1968
Document 834-00101-SR
NAS 8-21202

- 61) 1B-0450-61 Coatings for Solar Cells
Hoffman Science Center February 1961
Reorder No. 61-91
- 62) Brochure
Impleon News
Ion Physics Corp.
- 63) Doc 117921 17th Annual Power Sources Conference
Paper N64-17378
Large Area Solar Cells Prepared on Silicon Sheet
R. K. Riel and K. S. Tarneja
- 64) Doc 150,325-1 Development of Lightweight Rigid Solar Panels
EOS May 1966
TR 7027-1DR
- 65) Doc 157243-1 Review and Evaluation of Past Solar Cell
Development Efforts
RCA December 1966
NASW 1427
- 66) Doc. 169,927-1 Large Area Thin Film Solar Cells
Final Technical Summary Report
MH 30 June 1962
DA-36-039-SC 88981
- 67) Doc. 153,236-1 4 KW Solar Photovoltaic Power System Design
Study Final Report
Westinghouse ASD-TDR -62-158 January 1962
- 68) Doc. 158-497-1 Manned Mission Photovoltaic Power System Study
NAS 9-5266
Vol. -1
- 69) Doc. 158-498-1 Vol. -2
- 70) Doc. 158-499-1 Vol. -3
- 71) Solar Cell Space Manual
Central Lab.
El Monte, California

X

APPENDIX C
LIST OF MICROFILM REPORTS COLLECTED

PRECEDING PAGE BLANK NOT FILMED.

900-270

APPENDIX C

LIST OF MICROFILM REPORTS COLLECTED

N 62 - 11248

N 64 - 18388

N 65 - 19025

N 66 - 35946

N 66 - 24989

N 66 - 18407

N 65 - 18934

N 67 - 17867

N 66 - 22601

AD 469 - 960

AD 468 - 500

AD 817 - 614

AD 605 - 957

AD 400 - 636

AD 298 - 811

AD 406 - 818

AD 413 - 196

AD 427 - 268

AD 440 - 016

AD 443 - 496